TECHNICAL REPORT No. 29

OROGRAPHIC INFLUENCES ON MEDITERRANEAN LEE CYCLOGENESIS AND EUROPEAN BLOCKING IN A GLOBAL NUMERICAL MODEL

by

S. Tibaldi and A. Buzzi

February 1982

C O N T E N T S

ABSTRACT

The role of orographically induced cyclogenesis in the lee of the Alps in favouring the onset of Euro-Atlantic blocking is investigated by means of numerical simulations of a real case . The model used is the ECMWF global grid-point model as operational in August 1980. While the essential part that the local orography (the Alps) plays in triggering the development of cyclonic disturbances is confirmed for the first time using a global model, the relationship between Alpine cyclogenesis and European blocking remains less clear. The importance of global orography in generating and maintaining the blocking pattern is subsequently investigated and its crucial role evidenced and discussed.

1. INTRODUCTION

During the period of formation of blocking situations over Europe the Mediterranean is dominated, on average, by an area of relative depression, being affected by troughs or cut-off lows which are the counterpart of the high pressure that establishes itself over the north-eastern Atlantic or over Northern Europe.

In the various studies of blocking which have appeared in the literature, attention has mostly been devoted to the blocking anticyclone that develops and persists at high latitudes, rather than to the whole associated circulation. The reason is probably that the anticyclone has a more defined and persistent character ("centre of action") than the surrounding, more mobile, lows. However, from a dynamical point of view, it is not obvious that the role of these lows is secondary in importance for the establishment and maintenance of the blocking equilibrium.

In a recent paper, Illari, Malguzzi and Speranza (1980), hereafter referred to as IMS, point out that cyclogenesis in the Mediterranean assumes, in some

cases, the character of an "absolute" (or "in place") instability, resulting in the formation of stationary or slowly moving cut-off lows. This process is often associated with the breakdown of the westerlies over the Eastern Atlantic and Western Europe. The interruption of the mid-latitude westerly jet can, in turn, lead to a persistent blocking situation in the manner schematically described by Berggren, Bolin and Rossby (1949).

There is, therefore, some observational evidence of a connection between deep cyclonic formation over the Mediterranean and European blocking. Since a large number of cyclogeneses in the Western and Central Mediterranean are lee cyclogeneses caused or modified by the surrounding topography (Buzzi and Tibaldi, 1978, hereafter referred to as BT), we can also hypothesize an indirect link between the orography of Southern Europe (the Alps in particular) and European blocking. It is this aspect that originally prompted this work.

There are also some theoretical considerations that can suggest a link between absolute (in the IMS sense) cyclogenesis and blocking. A blocking situation is in general associated with anomalous amplitudes of the first few zonal wavenumber components in the middle troposphere (Austin, 1980), but it often appears also as a "local" (on the planetary scale) persistent disturbance, comparatively stable with respect to changes in upstream and downstream conditions. This means that the atmospheric state is in a locally stable state, possibly of the kind suggested by the solutions of McWilliams (1980, free modon), Trevisan and Buzzi (1980, solution with forcing) and Malguzzi and Speranza (1981, non-linear local resonance). In all of these cases the non-linearity plays an important role, and hence the shape is important in determining the equilibrium properties of the solution. In particular, McWilliams' and Malguzzi and Speranza's models reproduce the splitting of the jet typical of European blocking. It seems therefore

plausible that local disturbances which tend to establish a flow pattern (splitting of the jet, cut-off lows at middle-low latitudes) resembling that of blocking and in the right position (localized forcing being probably important) can lead to a proper blocking state, considering also that this state could have an "attracting" nature in the phase space of the atmospheric system (Charney and De Vore, 1979).

The dynamical problem of the entrance into a blocking situation is still open to theoretical and observational investigations. In this paper we describe how we try to gain some insight into these problems by means of numerical experiments on a real case of European blocking preceded by a deep cyclogenesis in the lee of the Alps. As more extensively reported below, the synoptic analysis suggests a link bet ween cyclogenesis and blocking, in the sense that the former seemed to have favoured the onset of the latter or, at least, controlled its shape and characteristics. A second aim of this work is to study the behaviour of a model designed for large scale simulation and prediction, in the presence of a phenomenon like lee cyclogenesis which is initiated by the action of a topographic obstacle (the Alps) whose scale is only marginally resolved by the model grid. If we should conclude that orographically induced cyclogenesis is relevant for the subsequent formation of blocking, we would have to face a typical problem of signal propagation from sub-synoptic scale to planetary scale, with possible implications on the importance of higher resolution modelling in NWP. The solution of this problem would require particular efforts to include the effects of steep orography of comparatively small horizontal scale.

We also report here about a preliminary result concerning the role of large scale orographic forcing producing and maintaining atmospheric blocking.

We choose, for our experiments, the N48 grid-point model in operation at the European Centre for Medium Range Weather Forecasts (ECMWF). It is a global

model and includes a rather sophisticated parameterization of physical effects: it is therefore suitable for describing planetary scale dynamics and perform realistic medium range (4 to 10 days) integrations. A satisfactory skill of this model in forecasting blocking has also been previously reported by Bengtsson (1980). The resolution of the ECMWF global model is also high enough (1.875 deg. regular lat/lon grid in the horizontal and 15 levels in the vertical) for the effect of the Alps to be described, at least to a simple extent.

2. THE CASE STUDY

The period of the case study embraces the last week of November and the first week of December 1978. The first three weeks of November were characterized by an almost zonal flow over the Atlantic and Europe, with the axis of the westerlies displaced in an anomalously northern position, so that the Mediterranean was dominated by anticyclonic conditions.

Between the 23rd and the 27th a dramatic change took place in the circulation over the Atlantic and Europe: a large amplitude trough-ridge system rapidly developed at 500 mb over respectively the east coast of North America and the middle Atlantic on the 24th and the 25th, and it was followed by a deepening of a downstream trough over Europe. The development of this latter trough was accompanied by a lee cyclogenesis that started between the 25th at 12GMT and the 26th at 00GMT over the Gulf of Genoa at low levels and evolved during the 28th and the 29th into a deep cyclone (the minimum pressure value being around 985 mb), moving very slowly south-eastwards in the central Mediterranean (see Figs. 1 and 2a to 6a). A corresponding cut-off low formed at 500 mb between the 27th and 28th and deepened further in the following 24 hours.

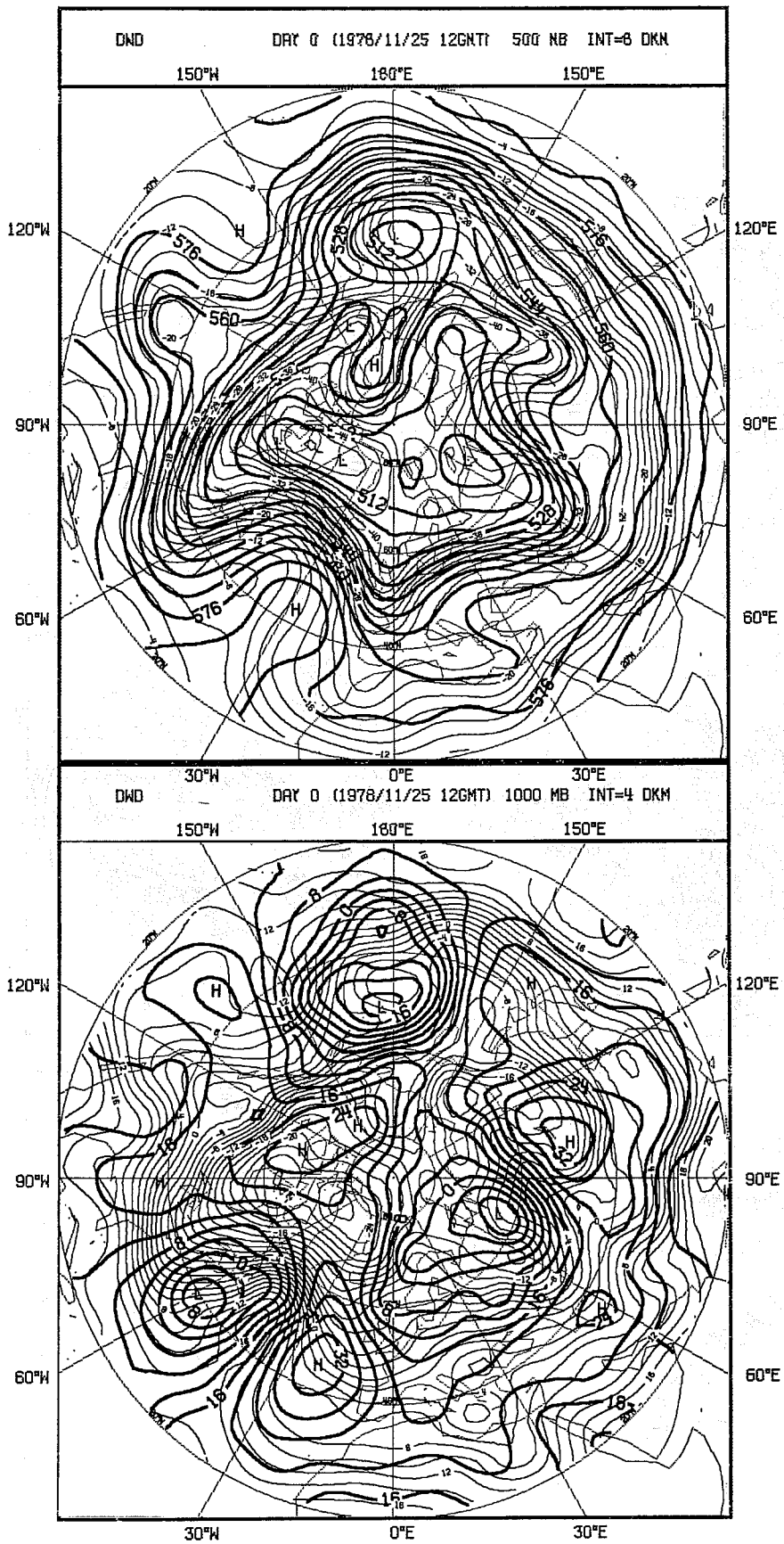

Fig. 1 Deutsche Wetterdienst analyses (top: 500 mb height and temperature, bottom: 1000 mb height and 850 mb temperature) for 12 GMT 25 November 1978. Initial conditions for all numerical experiments (Day 0). 500 mb heights drawn every 8 dkm, 1000 mb heights every 4 dkm. 500 mb and 850 mb temperatures drawn every 2°C.

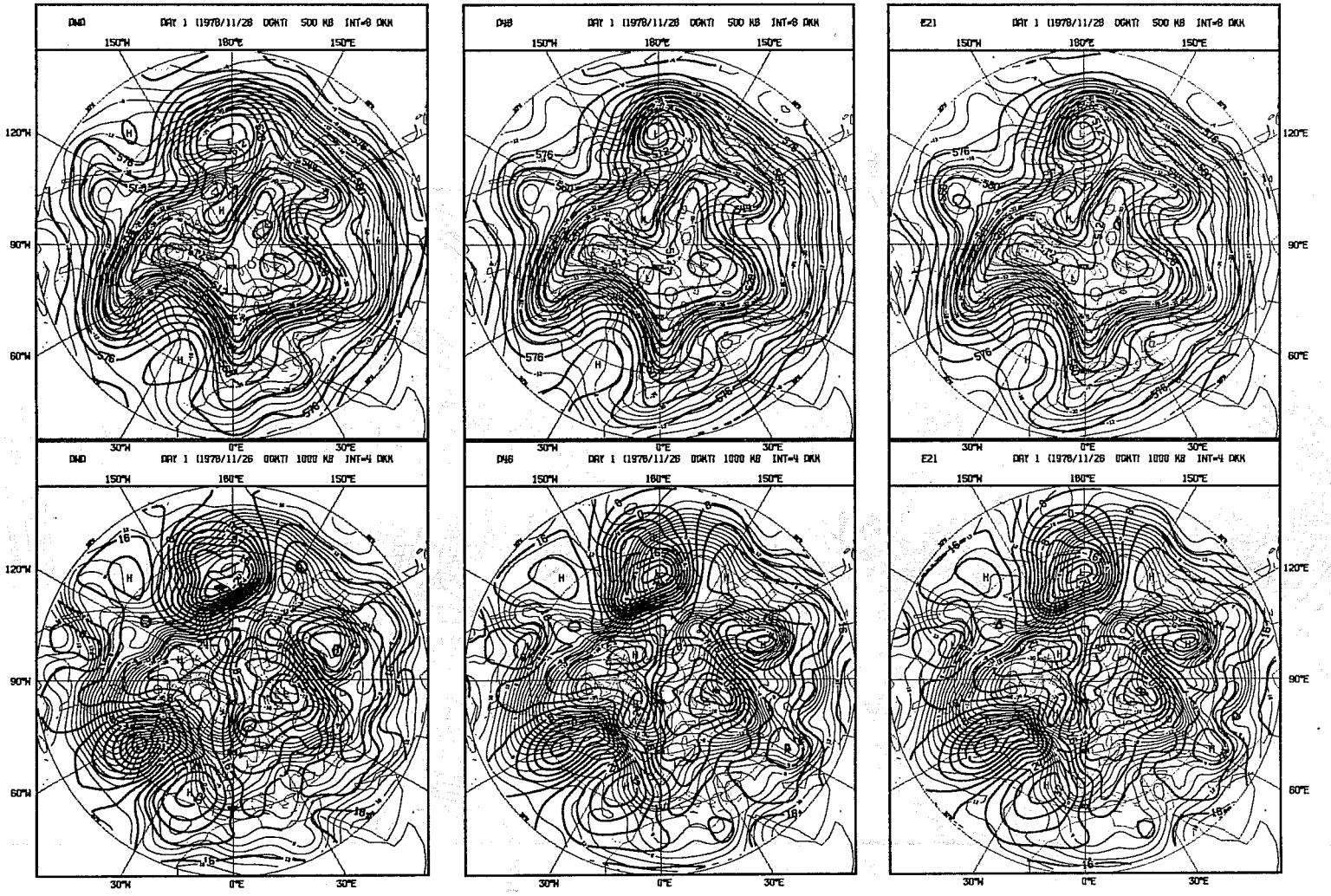

Fig. 2 (a): Same as Fig. 1, but for day ½ (00 GMT 26 November 1978).
(b): Same as (a) but for model run D46 (control).
(c): " " " " " " " E21 (enhanced Alps).

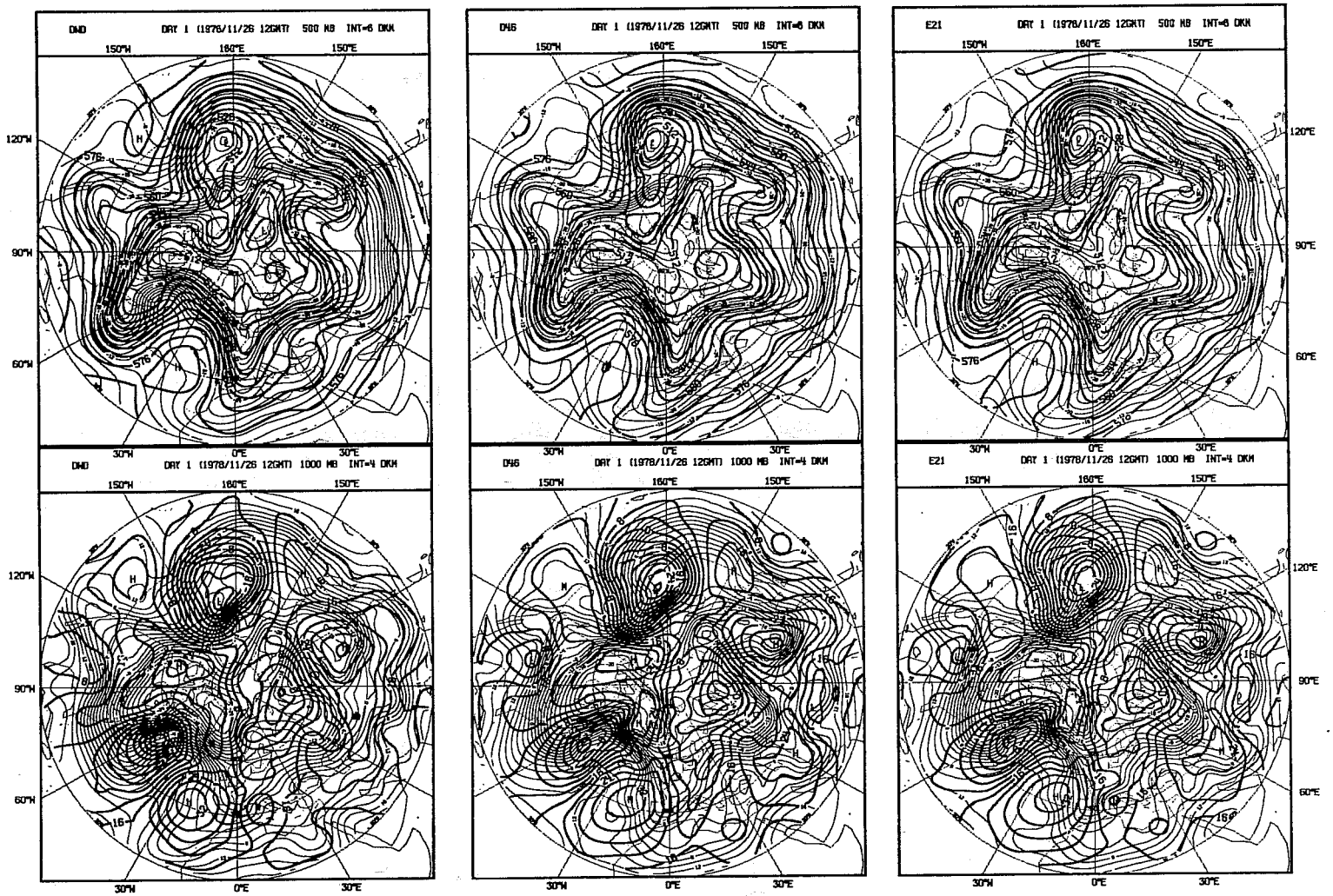

Fig. 3 Same as Fig. 2, but for day 1 (12 GMT 26 November 1978).

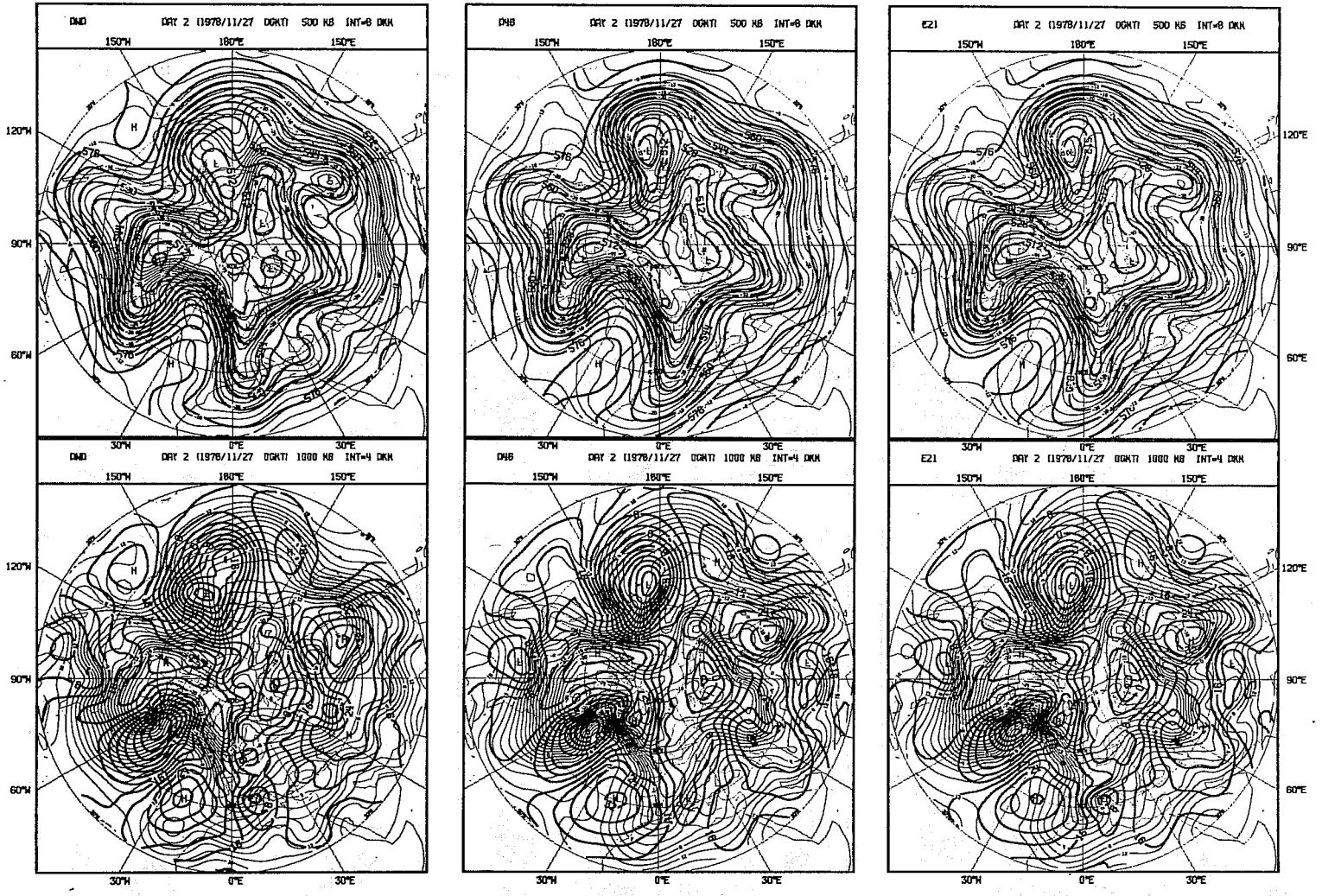

Fig. 4 Same as Fig. 2, but for day 1½ (00 GMT 27 November 1978).

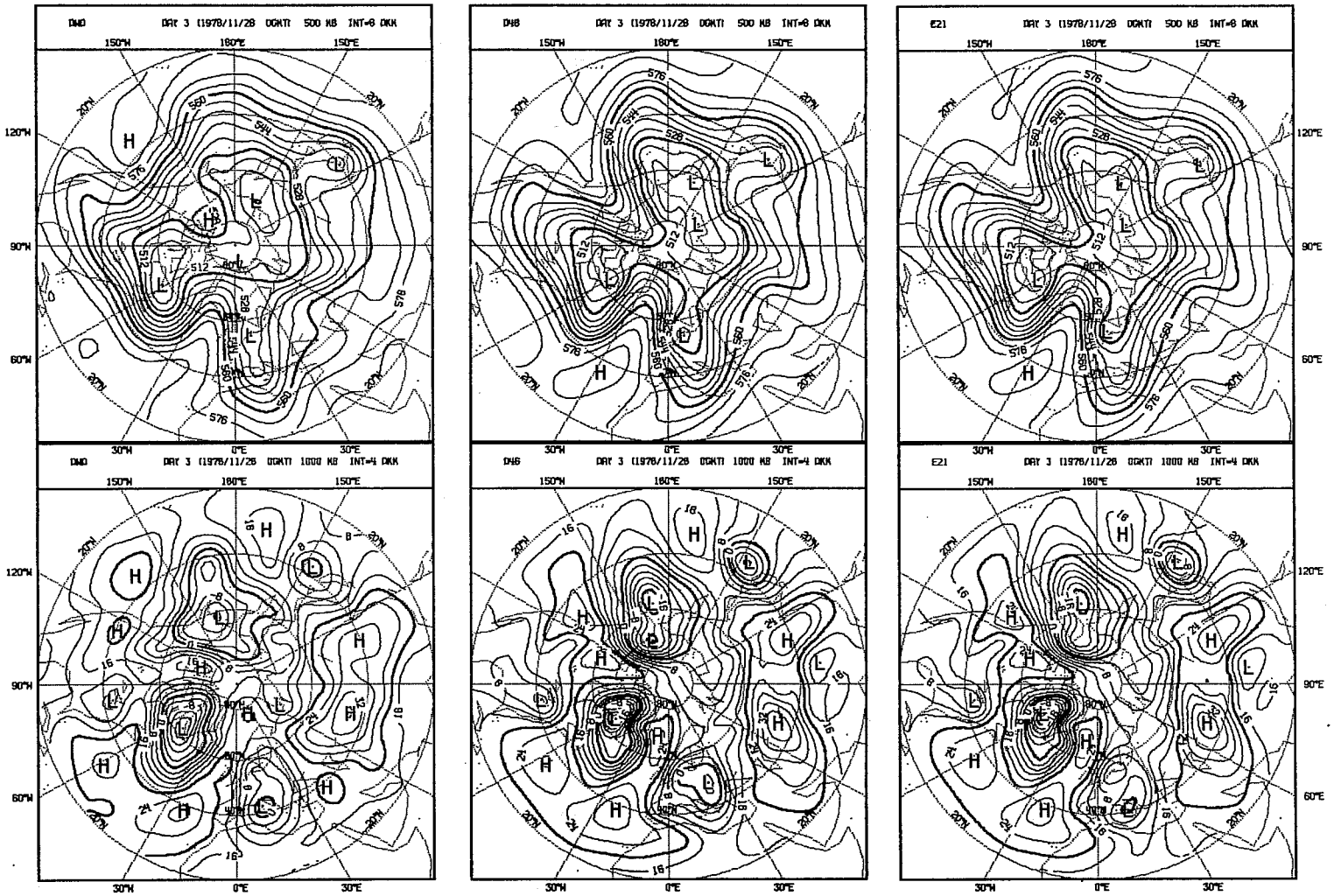

Fig. 5 Same as Fig. 2, but for day 3 (00 GMT 28 November 1978). Only heights are shown.

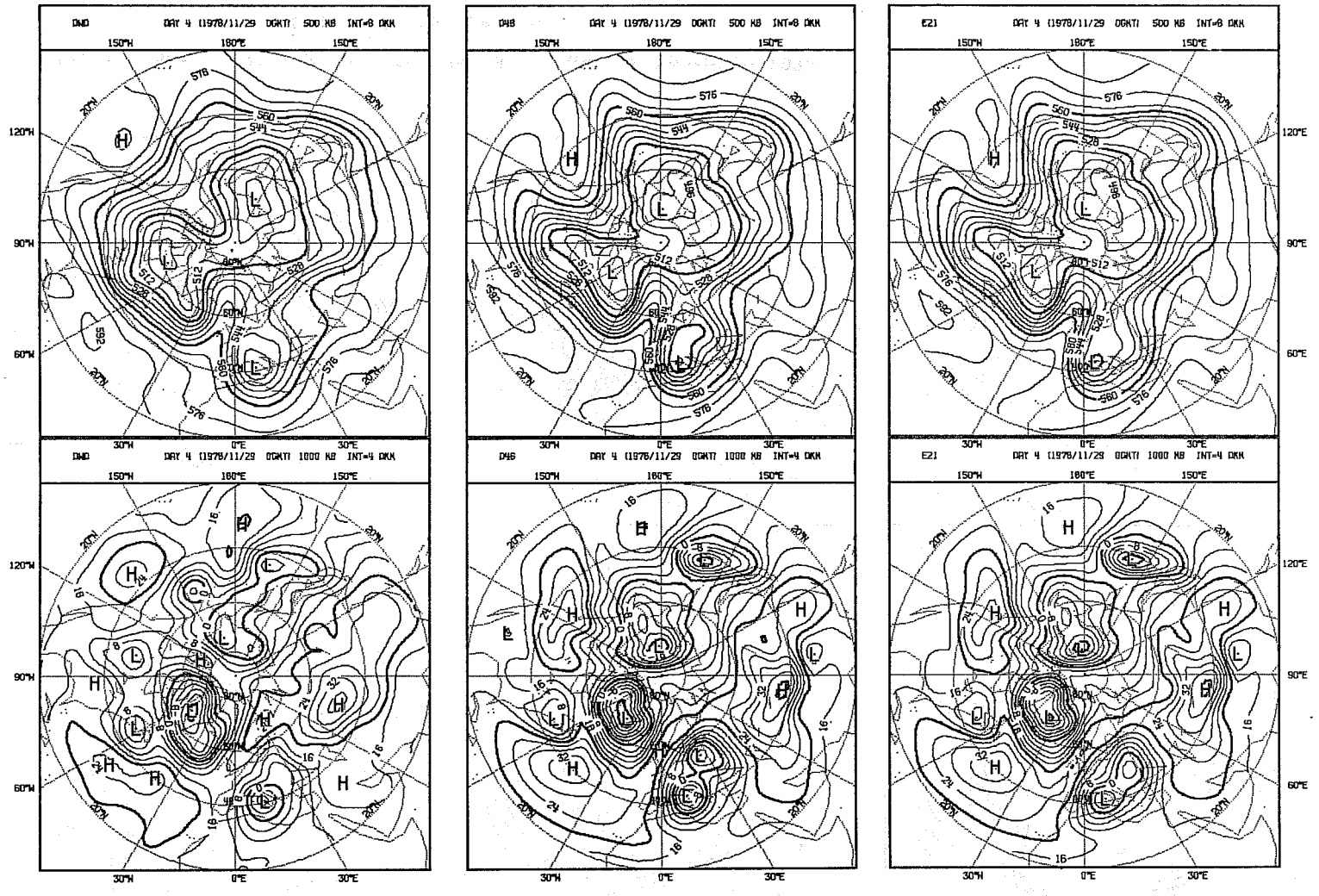

Fig. 6 Same as Fig. 5, but for day 4 (00 GMT 29 November 1978).

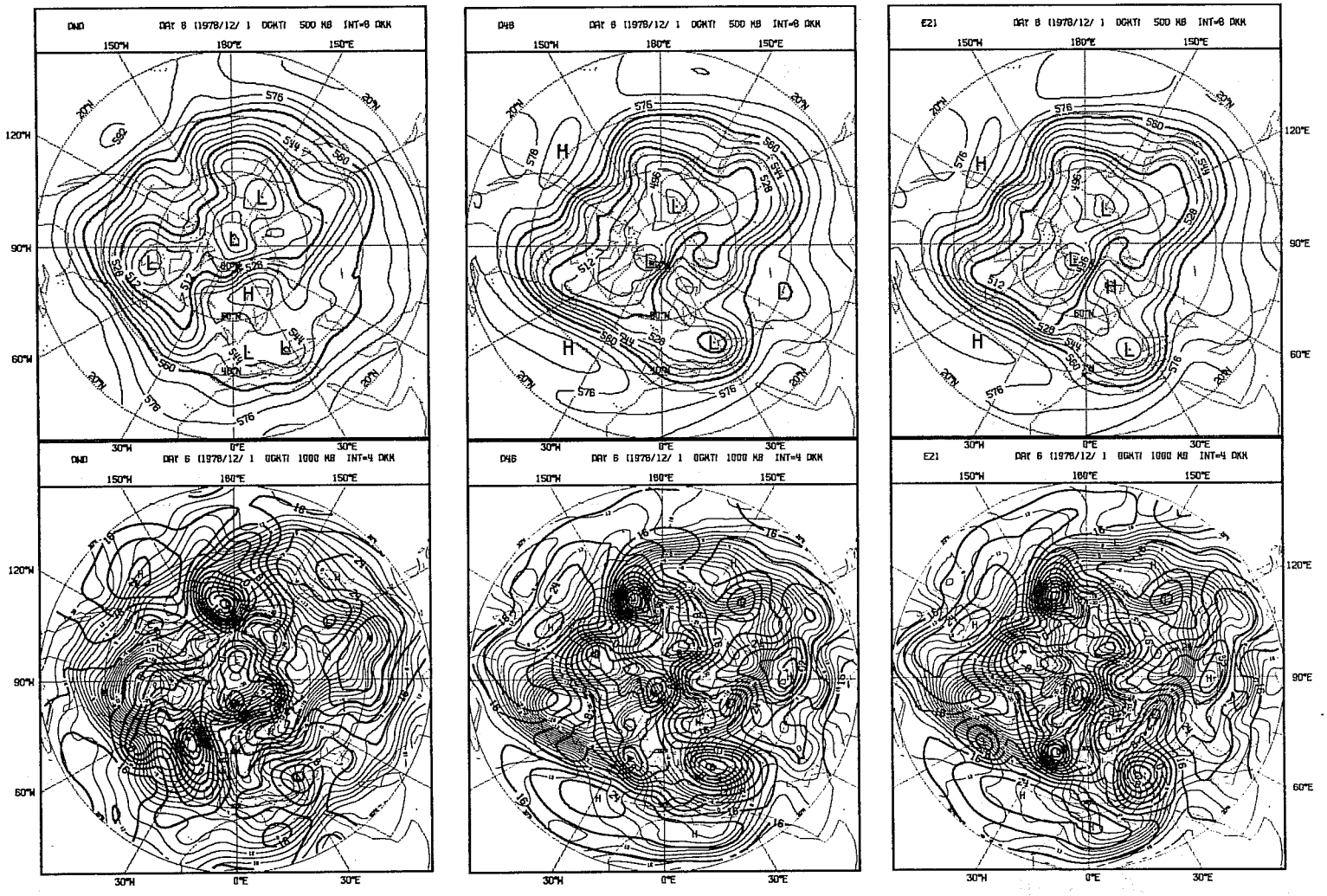

Fig. 7 Same as Fig. 5, but for day 6 (00 GMT 1 December 1978).

850 temperatures are shown overlapped with 1000 mb height maps (as for Fig. 1).

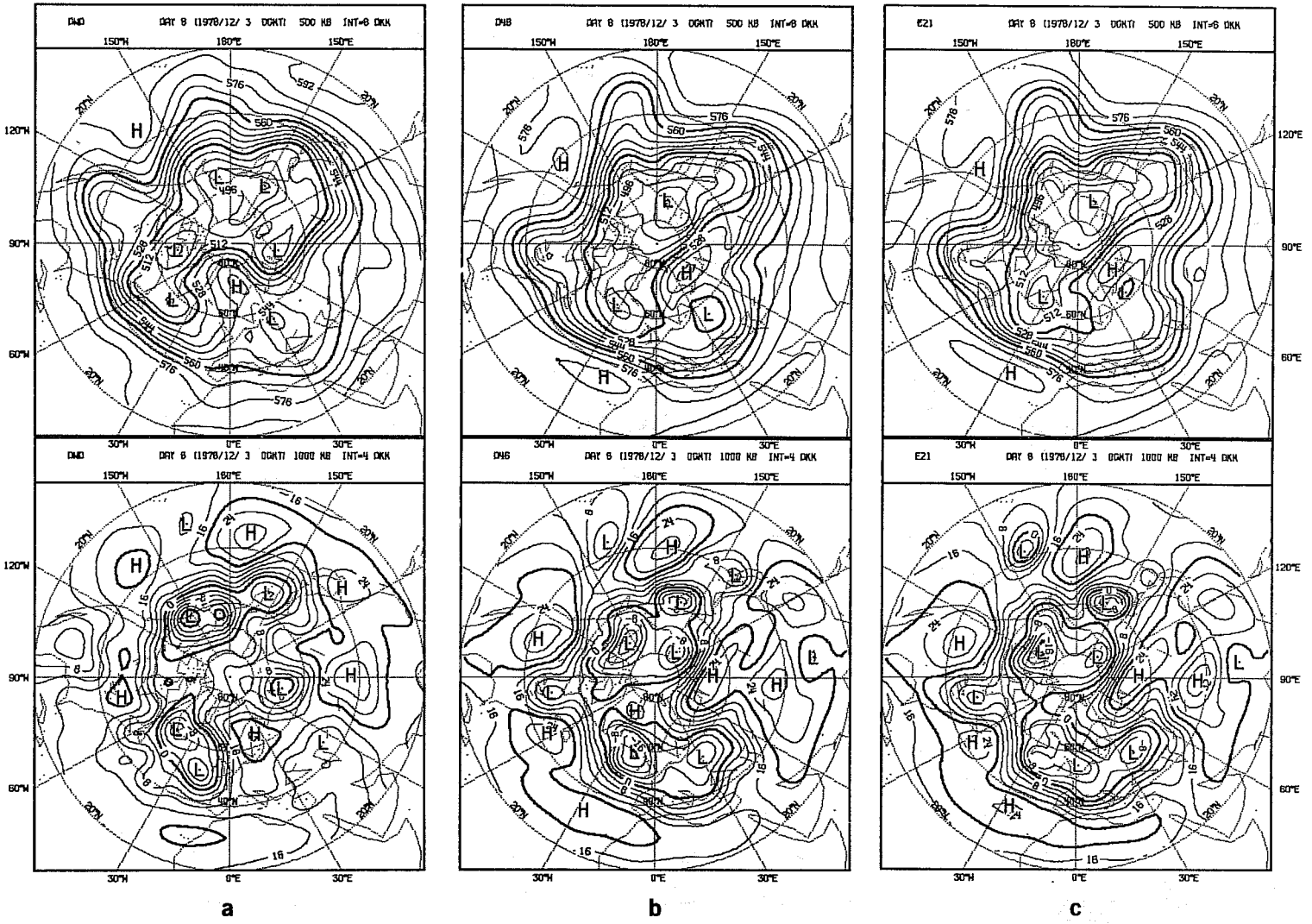

Fig. 8 Same as Fig. 5, but for day 8 (00 GMT 12 March 1978).

After the 29th at 00GMT, the Mediterranean cyclone drifted rapidly eastwards while filling, both near the surface and at high levels. It was in this stage, however, that the blocking circulation was set up over Europe. The process is better followed at 500 mb in Figs. 5a to 8a, upper parts: between the 28th at 00GMT and 29th at 00GMT the Atlantic ridge was "squeezed" between the almost stationary Mediterranean vortex and a new trough advancing eastwards in the Western Atlantic, so that an isolated blocking high formed on the 30th at 00GMT over the Norwegian Sea (figure not shown). At the same time the westerly jet split over the Atlantic at about 15 degrees west. The blocking circulation then assumed the characteristic omega shape and lasted, with little changes in shape or location, until the 11th.

The evolution of the lee cyclogenesis was consistent, at least in the first two days, with the schematic processes outlined in BT. The interaction of the cold front with the Alps produced the initial disturbance which then grew as a baroclinic disturbance. In Fig. 9 the intensity of the lee cyclone is plotted versus time. The intensity was computed by taking the average pressure difference between the centre of the cyclone and a surrounding circle of 1000 km radius. The longitude of the cyclone centre is also plotted to show the speed of its eastward propagation. This figure shows (for the moment only the graphs marked DWD will be of interest to us) that the initial disturbance (between the 25th at 12GMT and the 26th at 00GMT) grew rapidly, that is with an e-folding time of about 10 hours, and was followed by a period of slower growth (e-folding time of about 30 hours). After a period of very little development, from the 27th 00GMT to the 28th 00Z, a new growth phase can be identified during the following 24 hours. After the 29th at 00GMT, the intensity of the surface cyclone started to decline.

With regard to the displacement of the system during its life cycle, we observe that it grew almost in the same place both at the surface and at 500

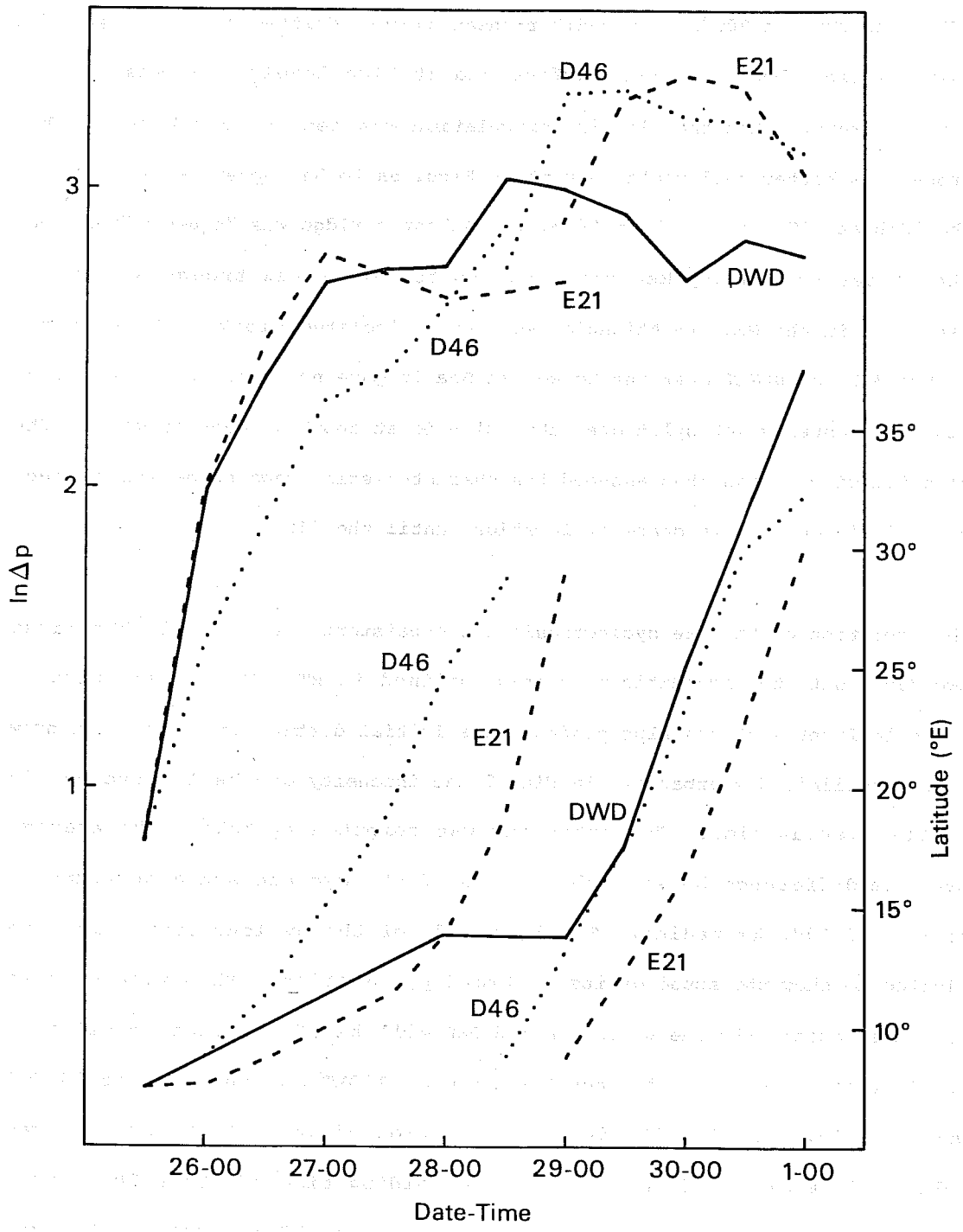

Fig. 9 Intensity of the pressure perturbation (upper set of graphs) associated with the cyclone centre in the lee of the Alps and longitudinal position of the cyclone centre (lower set of graphs) as functions of time (see also text).

mb, and only during the decay stage (after 29-00GMT) it drifted considerably eastwards. Following IMS, this cyclogenesis can therefore be classified as absolute. IMS give a criterion, based on the stability theory of barotropic Rossby waves, that allows to discriminate between absolute and convective instability. The criterion is based on the evaluation of the two parameters:

$$M=Uk^2/\beta \text{ and } N=uk^2/\beta$$

where U and k are respectively the horizontal phase velocity and wave number of the basic state Rossby wave, u is the basic state zonal wind and β is the local variation of the Coriolis parameter.

IMS' theory predicts then absolute instability, as opposed to convective, when the ratio M/N is larger than a critical value which depends on N itself and on the meridional wavelength of the Rossby wave. Although the validity of the theory is formally restricted to barotropic instability, the analysis of cases of cyclogenesis in the Mediterranean in terms of M and N, represented in Fig. 7 of IMS, reveals that the two regions of convective and absolute instability are well separated in the M,N plane. We have evaluated M and N for our case study, calculating these parameters as described in IMS, at 25-00GMT, that is before the initiation of the lee cyclogenesis. The values we obtained are M = 2.5 and N = 2.2, which situates this case well into the region of absolute instability. The value of M is even higher if computed on the 25th at 12GMT, that is just before the appearance of the lee cyclone. In conclusion, this case study was chosen for the following reasons:

1) a typical cyclogenesis occurred in the lee of the Alps

2) this cyclogenesis was intense, "absolute" in character and extended its influence to the whole of Southern Europe throughout the troposphere;

3) it coincided with the onset of a blocking circulation over Europe.

While the simple synoptic analysis does not allow to draw the conclusion that the cyclogenesis was a "cause" of the blocking, it suggests, however, the hypothesis, to be verified, that it played an important role in conditioning the process of blocking formation.

3. THE MODEL

The model used is the ECMWF global N48 grid-point model as in operation in August 1980.

The model uses the primitive equations on a global regular latitude-longitude grid of 1.875 x 1.875 degrees, it has therefore 48 grid intervals between the poles and the equator (hence the acronym N48) and 192 grid intervals along each line of latitude. The vertical coordinate is the well known sigma (p/p_{surf}) coordinate (Phillips, 1957). The vertical resolution is of 15 temperature and wind carrying levels, the uppermost being around 25 mb and the lowermost approximately $p_{surf}/20$ mb above the model's orography.

The (at the time) ECMWF operational model's orography was a substantially smoothed version (originally produced at GFDL) of Berkofsky and Bertoni (1955) orography (see Fig. 10).

The finite difference scheme is based on the staggered "C" grid, following Arakawa (Arakawa and Lamb, 1977). This grid was chosen, at the time, mainly because of its low computational noise and the ease of implementation of a

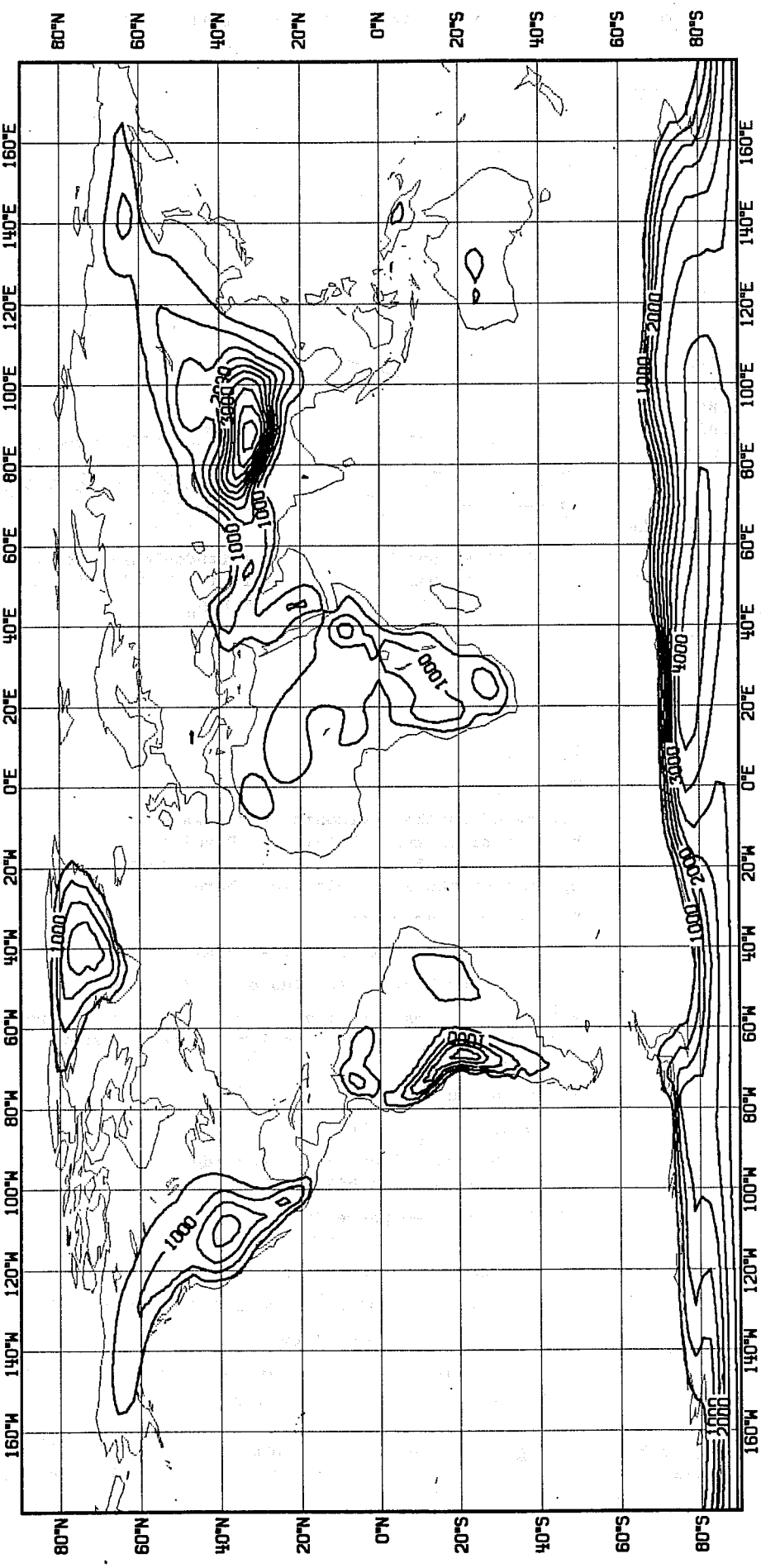

Fig. 10 ECMWF operational orography as at August 1980. This orography was used for the control experiment D46 and, except for the Alpine area, for experiment E21.

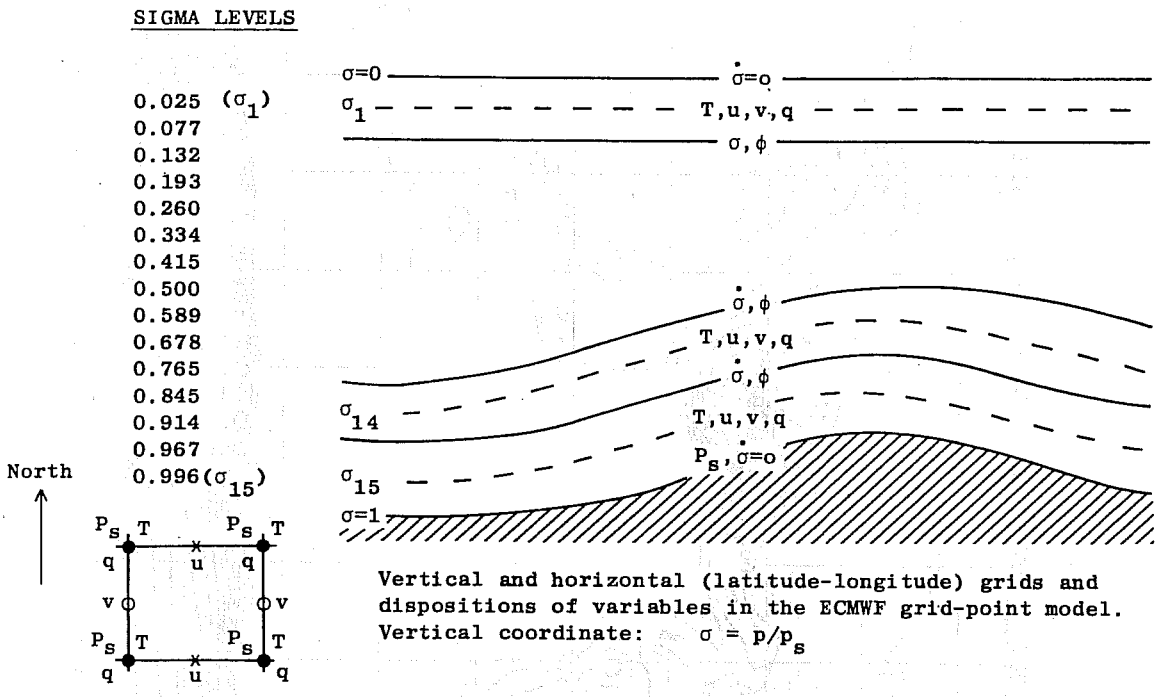

Vertical and horizontal (latitude-longitude) grids and dispositions of variables in the ECMWF grid-point model. Vertical coordinate: $\sigma = p/p_s$

Independent variables	λ, φ, ϕ, t
Dependent variables	T, u, v, q, p_s
Grid	Staggered in the horizontal (Arakawa C-grid). Uniform horizontal (regular lat/lon). Resolution: $\Delta\lambda = \Delta\phi = 1.875$ degrees lat/lon. Non-uniform vertical spacing of the 15 levels (see above).
Finite difference scheme	Second order accuracy.
Time-integration	Leapfrog, semi-implicit (Δt = 15 min) (time filter ν = 0.05)
Horizontal diffusion	Linear, fourth order (diffusion coefficient = 4.10^{15})
Earth surface	Albedo, roughness, soil moisture, snow and ice specified geographically. Albedo, soil moisture and snow time dependent.
Orography	Included, but very smooth.
Vertical boundary conditions	$\dot{\sigma}$ = 0 at p = p_s and p = 0.
Physical parameterisation	(i) Boundary eddy fluxes dependent on roughness length and local stability (Monin Obukov)
	(ii) Free-atmosphere turbulent fluxes dependent on mixing length and Richardson number
	(iii) Kuo convection scheme
	(iv) Full interaction between radiation and clouds
	(v) Full hydrological cycle
	(vi) Computed land temperature, no diurnal cycle
	(vii) Climatological sea-surface temperature

Fig. 11 Schematic table showing the principal characteristics of the ECMWF operational global grid-point model as at August 1980. This model was used in all simulations.

semi-implicit time scheme. Following the work of Arakawa (1966) and Sadourny (1975), the finite difference scheme was designed to conserve potential enstrophy during vorticity advection by the horizontal flow (the primitive equations being written in flux form). For more details on the adiabatic part of the model see Burridge and Haseler (1977) and Burridge (1979).

The parameterization of physical effects (the model's "physics") include a full hydrological cycle, a relatively detailed stability-dependent representation of boundary and free-atmospheric turbulent fluxes, and an interaction between the computed radiation field and model-generated clouds (Tiedtke et al, 1979). Fig. 11 contains a schematic lay-out of the model's characteristics.

The capability of the ECMWF global model to forecast a case of European blocking has already been reported and discussed by Bengtsson (1980). For more general information on the performance of the ECMWF model the reader is referred to Hollingsworth et al (1980).

4. DESCRIPTION OF THE EXPERIMENTS AND SYNOPTIC EVALUATIONS

Three significant experiments, consisting of 10 days of integration each, were executed, starting with the same initial condition and changing only the orography. In addition, two shorter experiments were run first to choose the optimal initial condition and to test the sensitivity of the integration with respect to it.

ECMWF analyses being unavailable for the period of interest, the US National Meteorological Center (NMC) global III-a analyses were used as initial conditions. The mass, wind and moisture data were interpolated from standard pressure levels to the model's sigma surfaces, then they were subjected to the ECMWF non-linear normal mode initialization (Temperton and Williamson,

1981 and Williamson and Temperton, 1981) before starting the model's integrations.

Since the cyclogenetic process started between the 25th at 12GMT and the 26th at 00GMT, the initial condition had to be chosen not after the 25th at 12GMT but, obviously, not too early in view of the aim of simulating the subsequent blocking process. Three preliminary runs of three days each, starting from the NMC analyses of 24-12GMT, 25-00GMT and 25-12GMT, showed that the integrations were similar to each other in the region of interest and therefore were comparatively stable with respect to changes in the initial condition. This was not the case in other simulations of Mediterranean cyclogenesis which showed a very critical dependence for the forecast of cyclogenesis and the related upper air trough evolution, on the instant chosen as initial state. However the existence of substantial discrepancies between the NMC and DWD (Deutscher Wetterdienst) surface analyses at 25-00GMT over the Western Mediterranean (probably in favour of DWD) suggested the choice of the latest time (25-12GMT) as initial condition for the 10 day runs.

The first experiment (D46) consisted in simply running the operational (August 1980) version of the ECMWF model. As mentioned in Section 3, the orography used by this version of the model is very smooth. Fig. 10 shows the global orography, while Fig. 12a shows an enlargement of the European area. It is immediately evident that the blocking effect of the Alps on the North Westerly cold outbreaks, which, as pointed out in BT, seems an essential mechanism to initiate cyclogenesis cannot be effective with this model orography.

The evolution of Exp. D46 is illustrated in Figs. 2b to 8b. The maps are directly verifiable comparing them with the corresponding DWD analyses just at their left.

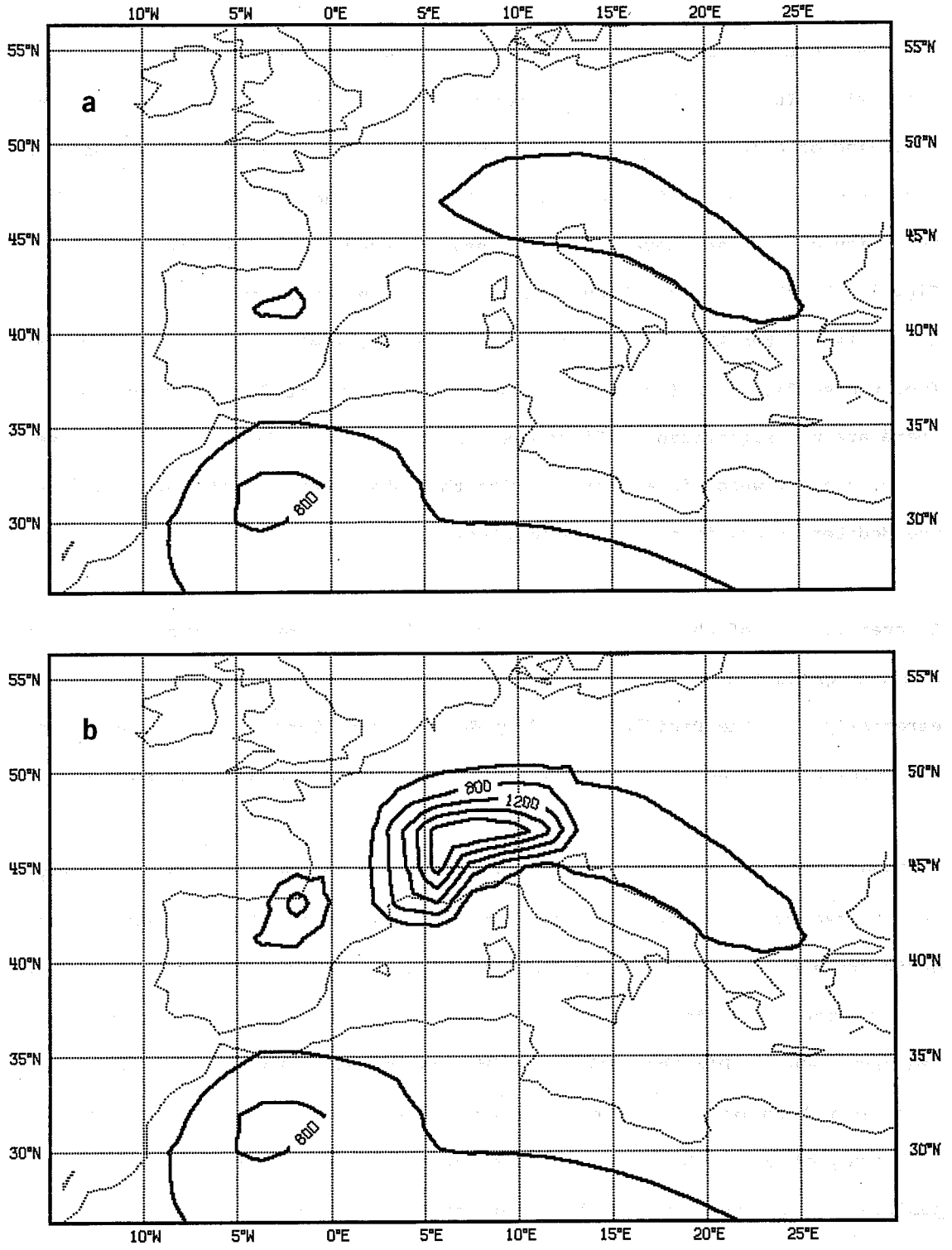

Fig. 12 (a) Enlargement over the European area of Fig. 10.

(b) Enlargement over the European area of the orography used in experiment E21.

At 26-00 the D46 forecast is generally good, as expected for a 12-hour prognosis. It is worth noting, however, that there is no evidence of the beginning of cold air blocking over the Alps that is observed in the analysis (note that the plotted isotherms are referred to the 850 mb surface). The intensity of the lee depression is already underestimated, as can be seen in Fig. 2. At 26-12 and 27-00 the failure of D46 in simulating the cyclogenesis in the lee of the Alps and the associated thermal field is becoming apparent from the surface maps (see Figs. 3 and 4) but, even at 500 mb over Europe, there are now significant differences. In particular, the jet splitting over France and UK, which is associated with the subsequent cut-off process over the Mediterranean, is not well simulated.

An overall view of the entire northern hemisphere reveals that there are other significant discrepancies between D46 and analysis at this time, especially over the Pacific, probably due to deficiencies in the original analysis, which lead to an early deterioration of the forecast in some areas.

At 28-00, (Fig. 5) the forecast over the whole of Southern and Eastern Europe is affected by the misrepresentation of the cyclogenetic process in the Mediterranean. While in the analysis the cyclone is centered over Italy at the surface and a deep trough is present at 500 mb over the Western Mediterranean, in D46 the cyclone, which has formed in the previous 24 hours over central Europe and Yugoslavia, is much shifted eastward. Also the southern portion of the European trough at 500 mb is to the east of its real position and too weak, while the development of the northern portion of it is overestimated. In order to evaluate better the subsequent evolution of the experiment, it is important to note that this second disturbance, associated with the northern portion of the European trough and characterized by a cold front and cyclonic vorticity advection aloft along the west side of the trough, later grows and, at 29-00, leads to a second cyclogenesis over the

Western Mediterranean, not due to the presence of the Alps, as shown in Fig. 6b. In Fig. 9, the intensity and longitudinal position of this new cyclone is reported in place of those of the old cyclone for D46 starting from 29-00. In the real development, only a trace of a second disturbance can be recognized, which reinforces the existing cyclone in the Mediterranean between 28-00 and 28-12, without substantially changing its location (see Figs. 5b and 6b). The result is that, at 29-00, the local forecast of D46 over the Mediterranean appears closer to verification than in the previous two days due to this spurious development. At 500 mb, the ridging process over the Eastern Atlantic and the cut-off over the Mediterranean are also satisfactorily simulated.

A major deficiency of the simulation appears, on the other hand, over the Pacific and North America, where the ridge-trough system in that region is overestimated. As said before, this failure appears to affect the subsequent downstream configuration and also the blocking formation over Europe. The forecast at days 6 and 8 are reported in Figs. 7 and 8 and show the evolution of the forecast during the second pentad.

The blocking configuration on December 1st at 00GMT is satisfactorily represented by D46 in the large-scale features, although the details are not captured, see Fig. 7b.For instance, the low over South-Eastern Europe is more intense than in reality, and the ridge over the Eastern Atlantic and the trough west of it are absent in D46. At 3-00, (Fig. 8b), the forecast has largely deteriorated, but a realistic blocking feature is still present in the model run, albeit in a more easterly position than in reality. The run was continued until 5-12, ,see Figs. 13a and 13b, when the blocking ridge, still present over Europe in the verification, has weakened substantially in D46 and drifted eastwards, around 40°-50° east.

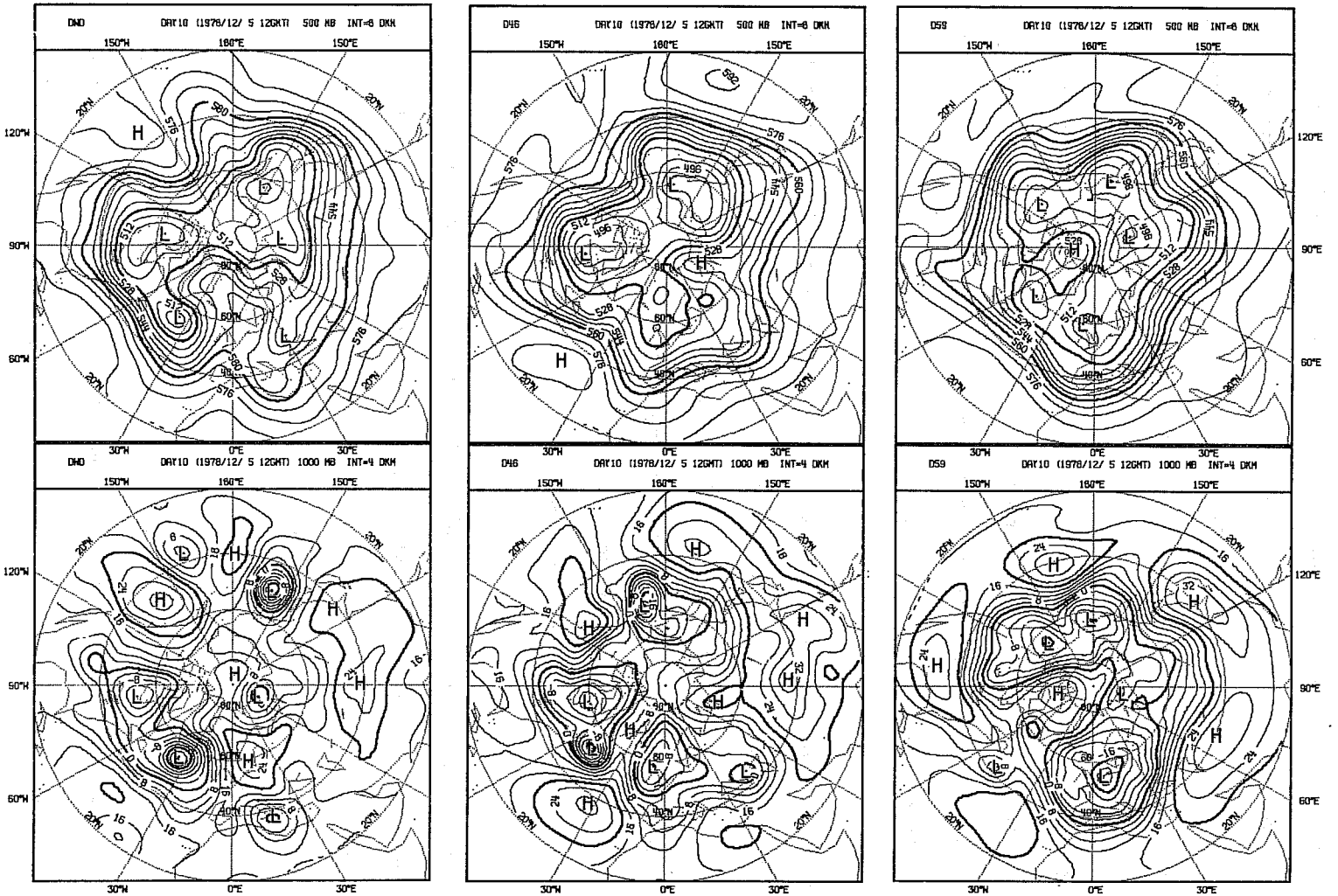

a b c

Fig. 13 (a): Same as Fig. 1, but for day 10 (12 GMT 5 December 1978).
(b): " " (a) but for model run D46 (control).
(c): " " " " " " " D59 (no mountains). Only geopotential heights are shown.

The second experiment (E21) differs from D46 only in that the local topography in the region of the Alps was arbitrarily modified. The new topography in the region is shown in Fig. 12b. It can be seen that the Alps are much enhanced in height with respect to the "operational" topography, reaching now a maximum of about 2500 m above msl; also the Pyrenees are made slightly higher. (A close examination of Fig. 12 will show that these enhanced Alps and Pyrenees are, in fact, displaced 1 grid point (1.875°) to the west. This was accidental and was realized only at a late stage of the work. It was decided not to rerun the experiment in view of the extreme smallness of the difference.) This artificial modification of the topography can be questionable. It is not the product of any objective operation on the real topography. Moreover, the dynamical and physical response of the model to such a steep obstacle of a horizontal scale near the margins of resolution is not obvious and can be subject to shortcomings. These new model Alps have been created only with the purpose of having an effective barrier, with maximum height closer to the average height of the "shadow" of the Alpine chain as would be projected on a vertical plane (which exceeds over 3000 m over a large fraction of the chain length). A main effect of this barrier on the oncoming flow in the presence of a cold front is that of hindering the horizontal advection in the lower layers, as pointed out in BT.

Previous numerical experiments (Bleck, 1977, Tibaldi, 1980, Tibaldi, Buzzi, Malguzzi, 1980) showed that the lee cyclogenesis phenomenon could be simulated in a rather realistic way, provided that the model Alps had height and steepness comparable to those prescribed here. The maps resulting from experiment E21 are shown in Fig. 2c to 8c. We can see that the cyclogenesis in the lee of the Alps, which was virtually absent in D46, is now reproduced.

On the 26th at 00GMT the frontal movement over the Alpine region is retarded. The phase of most rapid growth related to this frontal deformation, is very well simulated, as shown in Fig. 2c. The minimum pressure value, its

position and the temperature field at 850 mb, showing the cold air penetration over the Western Mediterranean and its blocking over the region south-east of the Alps, are predicted with very good accuracy. The pressure ridge north of the Alps is also simulated. Even at 500 mb the forecast is more realistic than in D46: the trough axis over the Western Mediterranean is more to the west than in D46 and the cut off process has already started. Twenty-four hours later (28-00, Fig. 4c) the E21 forecast is still definitely better than the D46 forecast over the region of interest, but later on, at 29-00, the two experiments tend to become more similar to each other, both showing two distinct cyclonic centres at the surface over Europe, while in the analysis only the cyclone over Italy (with a trough extending north-east of it) is present. The subjective evaluation still indicates that E21 is closer to the analysis than D46, and that the differences between the two experiments have spread over a larger region than before, affecting the whole European sector (see also next section). In particular the cyclone which is over North-eastern Europe in D46, is much weaker in E21 and is in a different position. In the same way the strong cyclone that is present in D46 over Italy and is the result, as seen previously, of a separate cyclogenetic process, is weaker in E21. This seems to confirm the hypothesis (see Tibaldi, Buzzi, Malguzzi, 1980) that an isolated obstacle like the Alps tends, in general, to hinder the larger scale baroclinic development, in spite of the fact that, in special circumstances, they can trigger and localize an initially smaller scale lee cyclogenesis.

The intercomparison of D46 and E21 on December 1, at 00GMT, i.e. during the stages of formation of blocking, can give information about the role of the Alps and the induced cyclogenesis on the blocking itself. Two things have to be remembered before commenting on the results. First, the blocking is a large scale phenomenon in nature, and is influenced by many factors (Bengtsson, 1980); therefore all the shortcomings affecting experiment D46,

except for the presence of the Alps, also affect experiment E21. Second, the spurious cyclogenesis occurring over the Western Mediterranean at 29-00 in D46 (see Fig. 6), and, to a lesser extent, also in E21, can shield the effects of the previous lee cyclogenesis that is observed in the verification. Actually, both experiments at 1-00 (see Fig. 7) show to some extent a stronger cyclonic circulation over Eastern Europe than observed, as a consequence of the spurious cyclogeneis. For the above reasons it cannot be expected that experiment E21 should perform substantially better than D46 at this later time. Nevertheless, the differences in the European sector between the two experiments are still in favour of E21; they are: a) the smaller intensity in E21, and the more precise position (at the surface) of the cyclonic centre over South-eastern Europe; b) the more pronounced ridge over Spain and Western Europe that stretches towards the high latitude blocking anticyclone; c) the temperature field at 850 mb that in E21 protrudes from Scandinavia towards Italy, while in D46 it is shifted too much towards the Eastern Mediterranean.

The maps at 3-00, see Fig. 8, are probably too far from the initial condition (eight days of integration) to derive any firm conclusions from the intercomparison between the two experiments. It is interesting to note, however, that significant differences can be observed all over the Northern Hemisphere. These differences, at least those very far from the Alps, are not to be interpreted mainly as dynamically induced Rossby modes excited by the Alps but rather as the result both of propagation of gravity-inertia waves moving away from the Alps and of the growth, due to the natural instability of the model atmosphere, of very small changes introduced everywhere by the non-linear normal mode initialization procedure in response to the local change of the topography.

The last experiment was done in order to evaluate the impact of the global orography on the onset and maintenance of the blocking. There is a general

consensus in the literature on the importance of the Earth's orography in controlling the behaviour of the long waves, and in particular of their stationary component. The mechanisms of generation of the long waves through the topographic forcing and topographic catalization of instability have not been fully clarified and are the object of current investigations (see, for example, Charney and Straus, 1980). It is very likely, in any case, that blocking cannot be properly modelled and simulated if the orographic forcing is neglected. This hypothesis is supported by the outcome of experiment D59, which consists of a 10-day run differing from the previous two only in that the Earth surface was flattened everywhere (the land-sea physical differences were however, maintained). The evolution of experiment D59 is shown in Fig. 14a to c (days 2, 4 and 6), and day 10 is shown in Fig. 13e, where it can be compared directly with D46 and with the verifying analysis.

At 27-00 (Fig. 14a), the forecast does not differ much from E21 and D46, except in regions of extensive mountain complexes, like, for instance, the Himalayas. However the cyclogenesis in the lee of the Alps is completely missing. At 29-00 (Fig. 14b) the large scale forecast still preserves some realistic features, particularly in the European sector, where the trough-ridge system, that developed later in the verification into the blocking pattern, is, at this time, apparently predicted not substantially worse than in E21. Nonetheless, over the large continental areas (Asia and North America) the forecast is rapidly deteriorating. This deterioration soon affects the blocking formation over Europe. In fact between 29-00 and 1-00 the Atlantic ridge, instead of tilting and producing a cut-off high over Scandinavia, gradually disappears. As a consequence a zonal flow reestablishes itself over the Atlantic and Europe, with superimposed short disturbances travelling eastwards (see Fig. 14c). Fig. 15 shows Hovmöller diagrams for the wavenumber band 1 to 3 for the control experiment D46, the no-mountain experiment D59 and for the verifying analyses. It can be seen

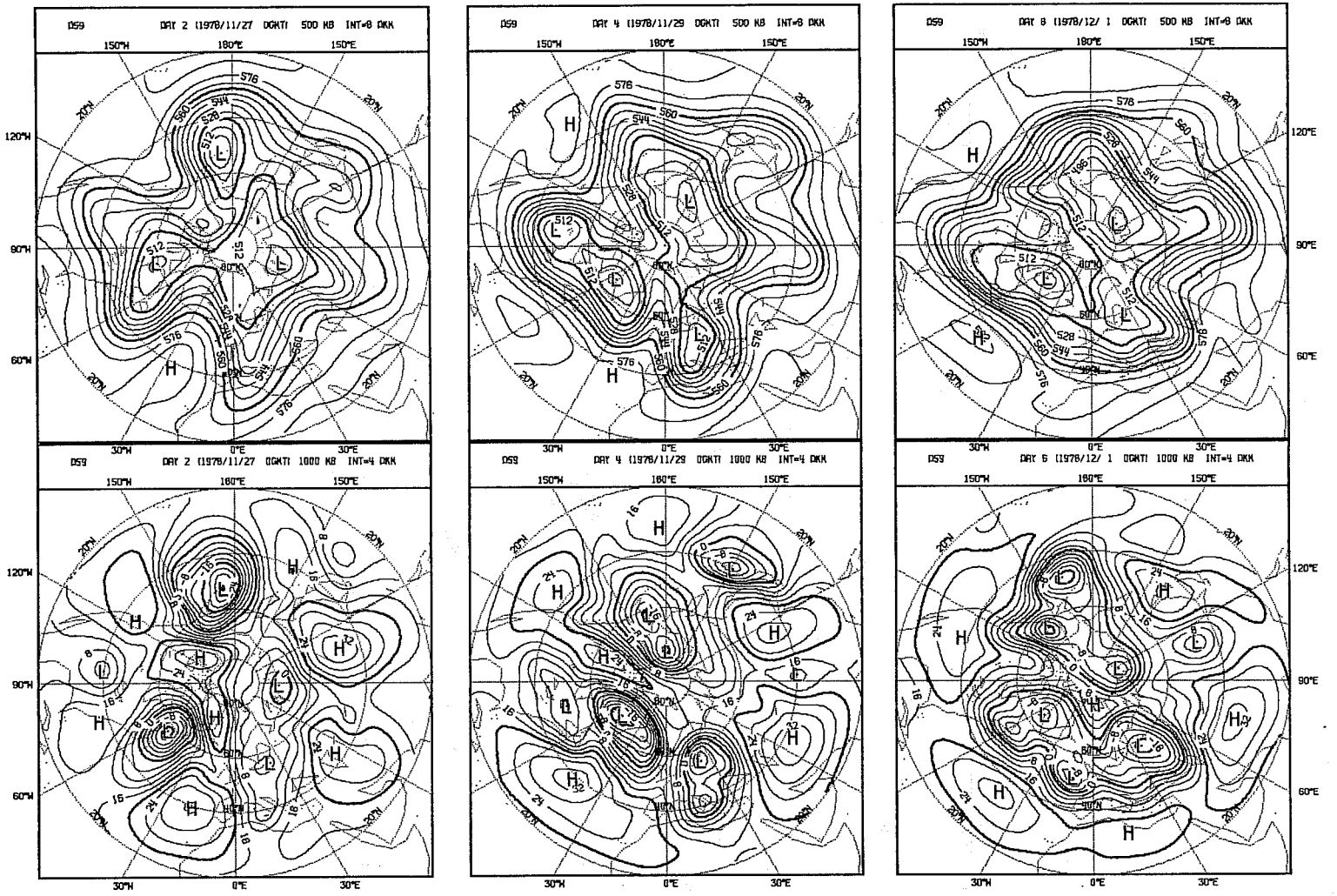

Fig. 14 (a): Same as Fig. 1, but for day 2 of model run D59 (no mountains).
(b): " " " " " " " 4 " " " " " " Only geopotential heights are shown.
(c): " " " " " " " 6 " " " " " "

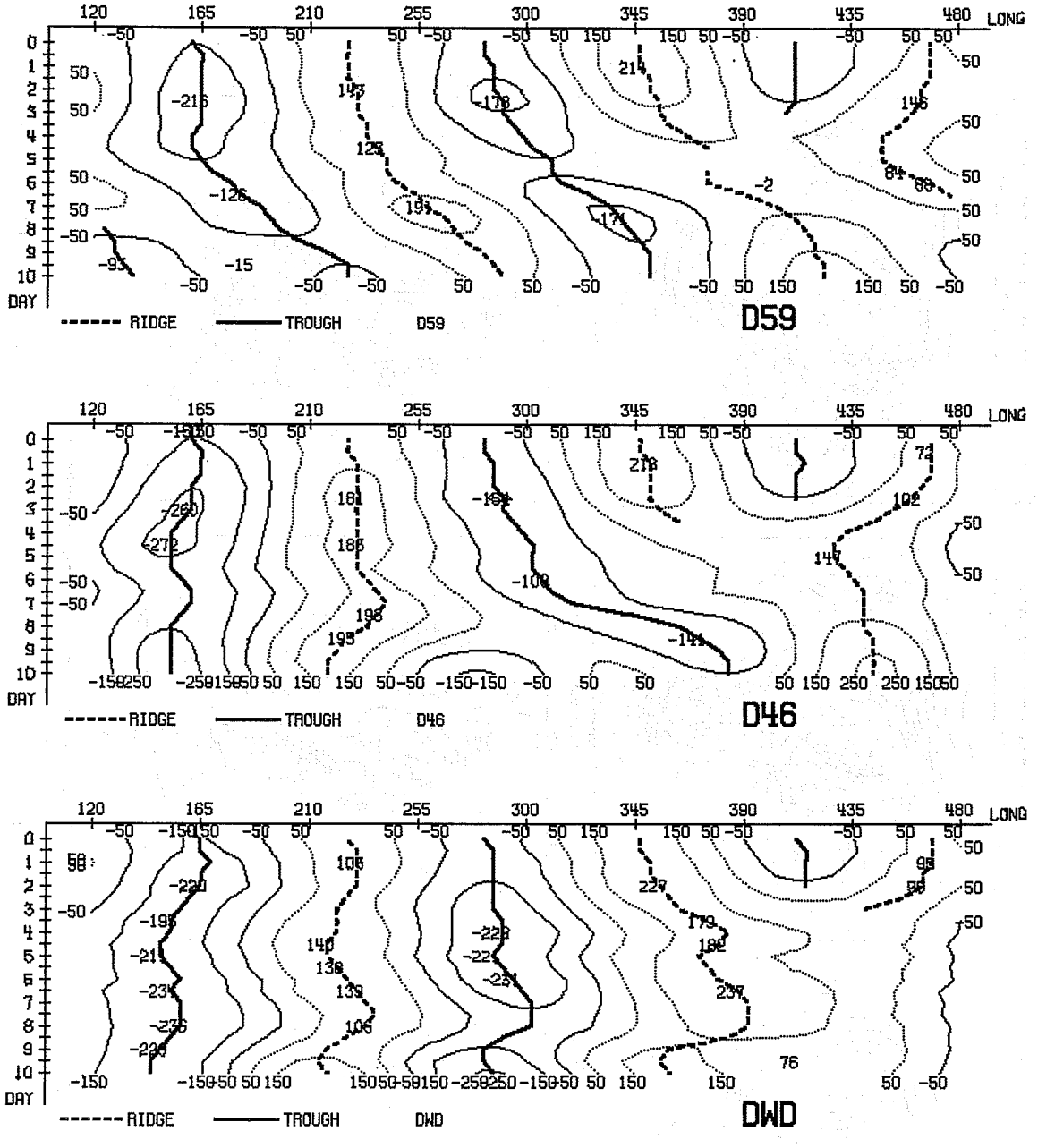

Fig. 15 Hovmöller diagrams for wavenumber 1 to 3 waveband - isolines of 500 mb geopotential height as a function of time and longitude. DWD: verifying analysis. D46: control run. D59: no mountains run.

clearly from these diagrams that the quasi-stationary troughs and ridges well identifiable almost all around the globe (165°E, 230°E, 230°E, 345°E) are correctly treated as almost stationary by the control run (with the only exception of the trough at 280°E). The no-mountain run, on the other hand, tends to treat the ultra-long modes as eastward-propagating, because of the absence of the stationary forcing represented by the orography. This effect is particularly evident from day 4 onwards.

Fig. 16 shows the spectrum of kinetic energy for the troposphere, averaged during the last 5 days of integration. It is evident how D46 and E21 behave similarly to each other and to the verification (at least in the overall spectral distribution), with D59 showing an altogether different signature, with much less energy in the ultra-long waves and a spurious peak in wavenumber five. The effect of the lack of large scale orographic forcing is again evident.

It is interesting to note that not all of the Northern Hemisphere flow becomes zonal as a consequence of the elimination of the topography. A sort of blocking ridge appears near the west coast of North America in the first few days of integration of D59, see Fig. 14 ,developing from a ridge present in the initial analysis, and slowly drifts eastwards for the entire period of the experiment (unlike experiment D46 and the verification, see Fig. 13). This fact could be tentatively taken as an indication that the orographic forcing is not essential to produce all kinds of blocking patterns, thermal forcing or the formation of a modon-type structure (McWilliams, 1980) being other possible explanations for these phenomena.

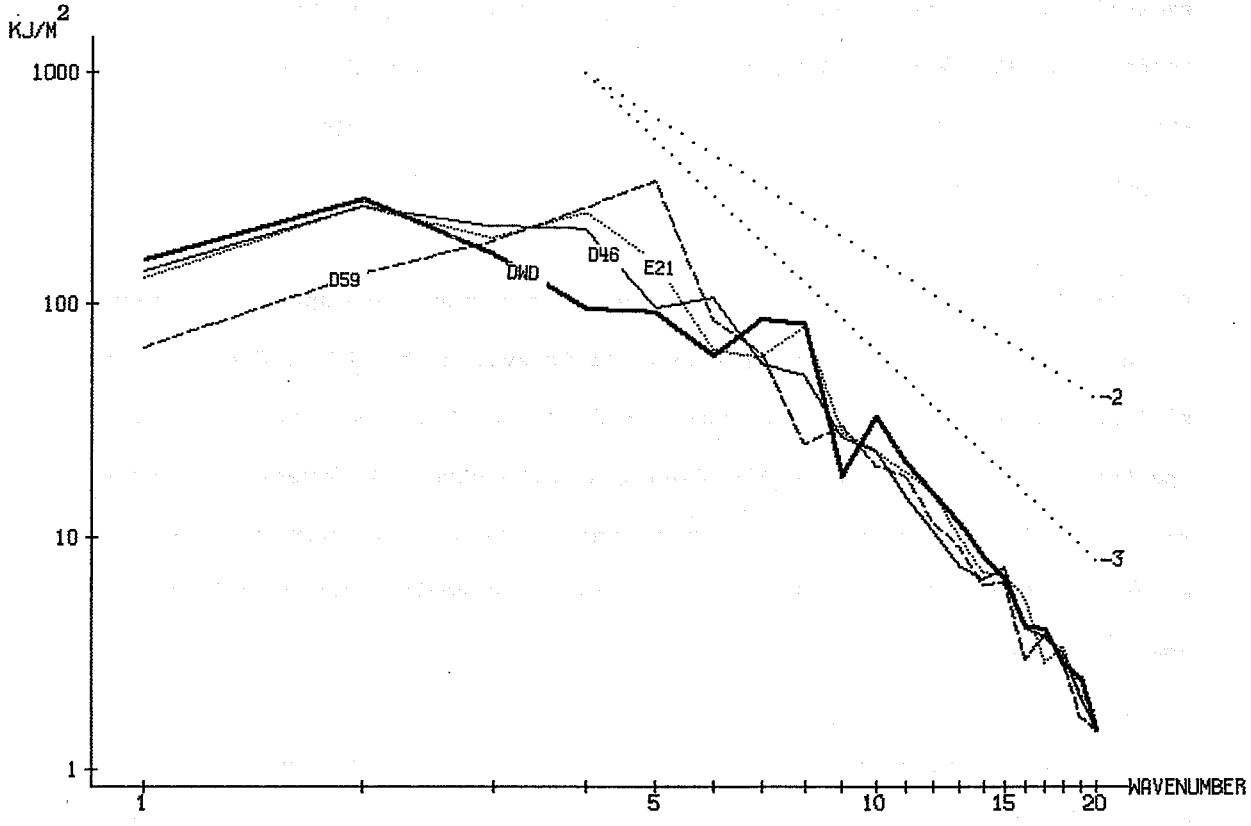

Fig. 16 Spectrum of average geostrophic kinetic energy (KJ/M^2). Average performed in time between day 5 and day 10 and in space between $40^{o}N$ and $60^{o}N$ and over the whole tropospheric depth.

5. SOME CONSIDERATIONS ON THE ROLE OF OROGRAPHY

These numerical experiments confirm that neither lee cyclogenesis in the Mediterrranean nor European blocking can be successfully forecasted without properly taking into account the forcing due to orography. The importance of a comparatively small-scale orographic feature like the Alps in modelling this sort of weather development is clearly shown in Fig. 17, where the 1000 mb height 5 day mean maps for the first half of the integrations are shown. While experiment E21 is the only simulation that gives a satisfactory synoptic picture of the circulation over Europe (Fig. 17c), the control run D46 essentially behaves, in this region, like the no-mountain run D59 (Figs. 17b and 17d respectively). This also shows that the effect of a "sudden disappearance" of the large-scale orographic forcing (this is, in fact, what D59 experiment ultimately means) needs a few days to impact on the model's circulation of the global atmosphere.

The importance of the large-scale orography in determining the onset and the conditions for maintenance of the block, and of the large-scale circulation in general, is clearly summarized in Figs. 18 and 19. They show, respectively, the 500 mb and 1000 mb 5 day mean height maps from day 5 to day 10 of the integrations. Experiments D46 and E21 show essentially the same behaviour during this second half of the integration period, producing, both at 500 and 1000 mb, a fairly satisfactory forecast of the 5 day mean maps, albeit the ridge associated to the European blocking doublet being largely underestimated and displaced in emphasis towards the north-east. The southerly branch of the split-jet is, accordingly, wrongly emphasized with respect to the northerly portion, in reality much stronger. All other main troughs in the northern hemisphere are also predicted satisfactorily, possibly with the exception of the ridge-trough system over the Rockies and the North American continent which is forecasted 20° to 30° too much to the east of the observed position. D59, conversely, shows no signs of blocking doublet, replacing it with a huge, double-structured, trough that occupies

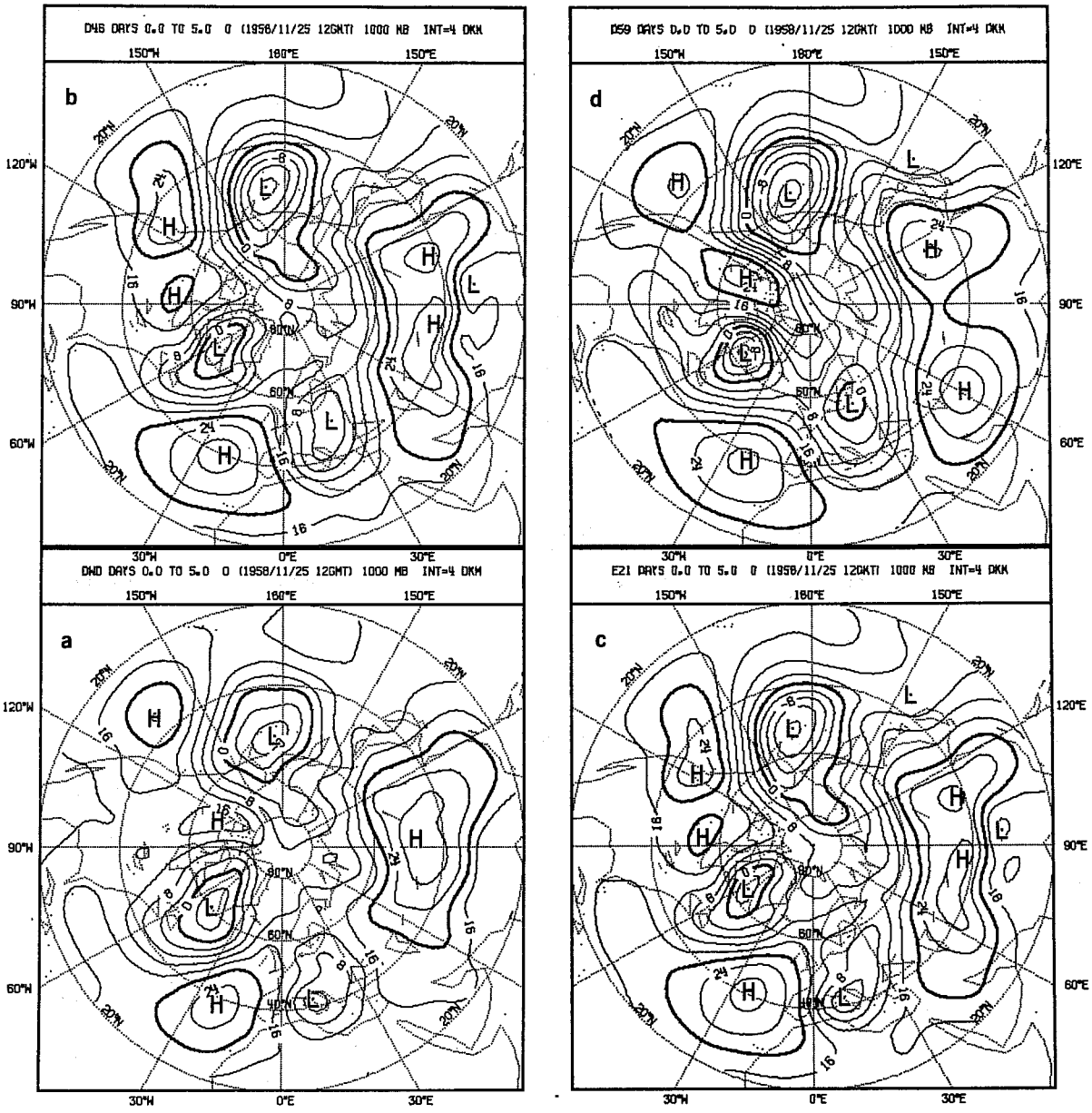

Fig. 17 (a): 1000 mb geopotential height observed 5 day mean map, day 0 to 5.
(b): as (a) but for experiment D46 (control).
(c): " " " " " E21 (enhanced Alps).
(d): " " " " " D59 (no mountains).

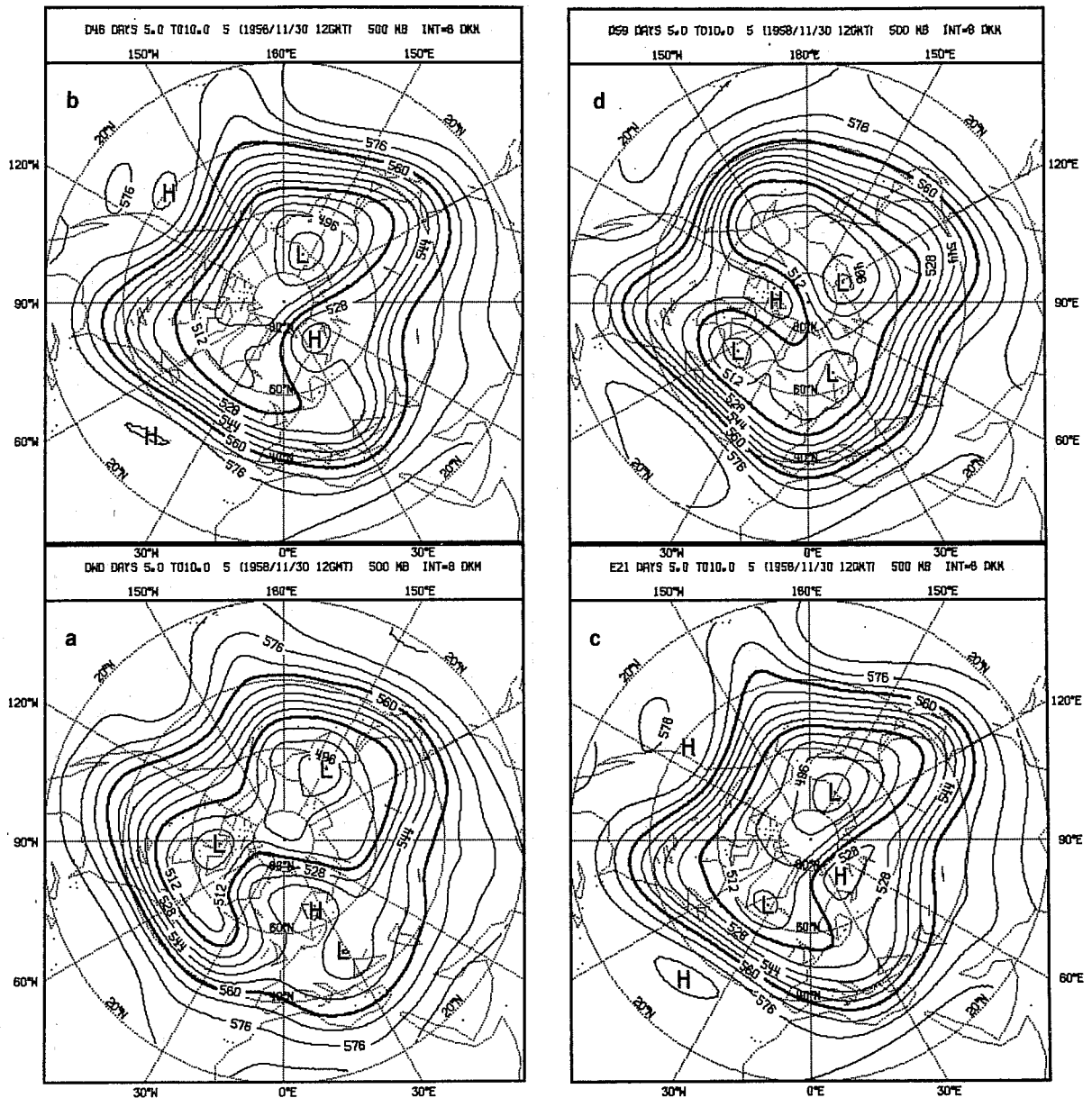

Fig. 18 As Fig. 17 but for 500 mb geopotential height and for day 5 to 10.

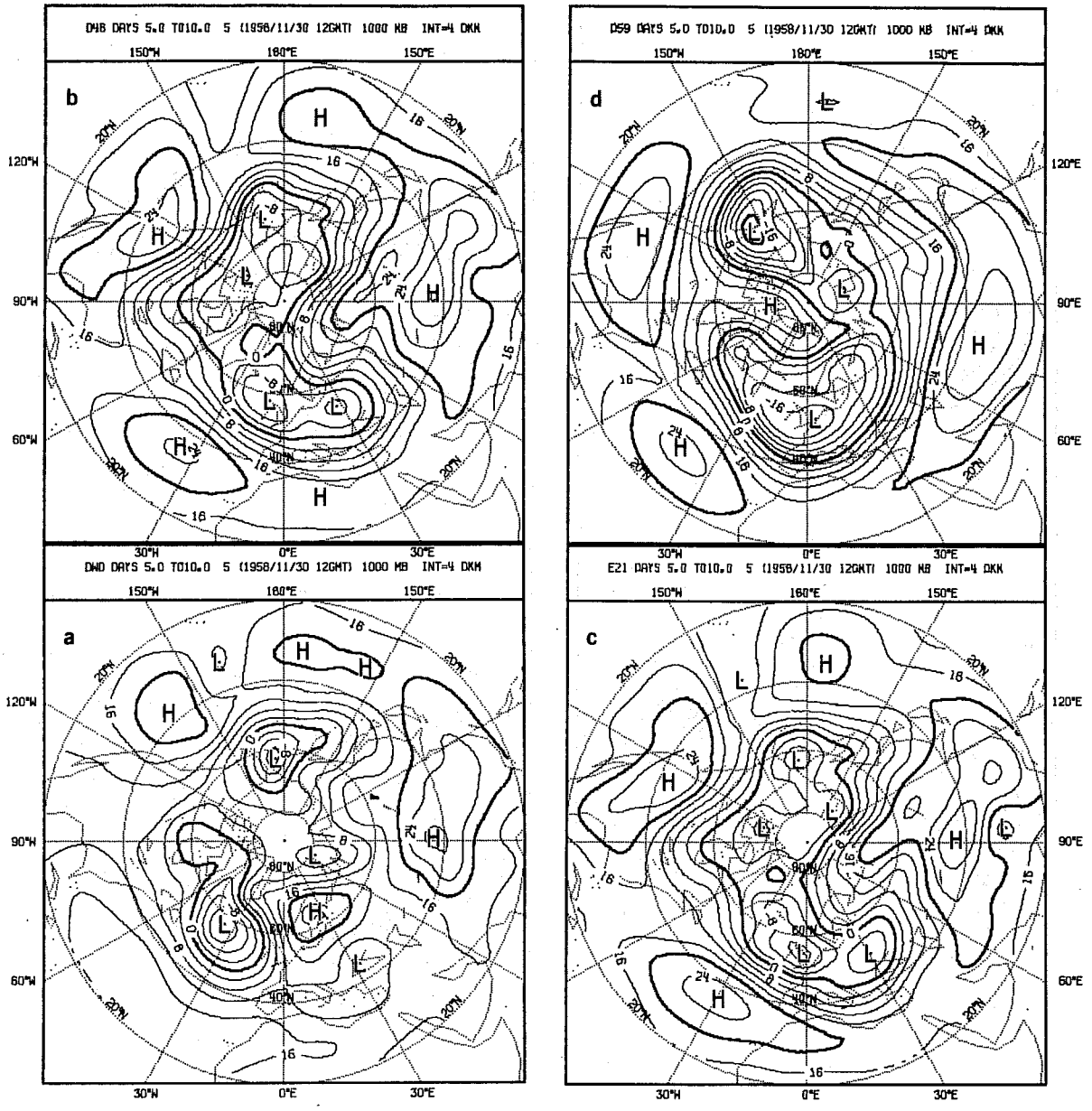

Fig. 19 As Fig. 18 but for 1000 mb geopotential height.

the whole quadrant 30°W-60°E. The western hemisphere circulation is disrupted almost everywhere and all major large-scale features are heavily out of phase.

Turning our attention to the comparatively smaller differences between experiments D46 and E21, some interesting considerations can be made about the role of the Alps on European meteorology. Due to the relatively local nature of these differences, the objective scores available in the ECMWF Research Department diagnostic package, designed as they are to assess the performance of experiments over a hemispheric scale, are not the most suitable tool for our particular purpose: Fig. 20 shows, however, that from this "hemispheric" point of view, the overall best is the control run D46, with E21 slightly worse, but showing overall little difference and D59 (the no-mountains run) coming a poor third with much lower scores.

Better for our purposes are the difference maps. Fig. 21a shows 5 day mean difference maps E21-D46 averaged over the first half of the experiments (day 0 to day 5), lower part showing 1000 mb height and upper 500 mb height. Fig. 21b shows the same, but for day 2 only. These maps illustrate the character of the disturbance produced by the enhanced model Alps: it has a dipole structure confined near the mountain, but with a horizontal scale much larger than the mountain itself. Besides the low centre south of the Alps, a high centre of comparable amplitude is evident to the north (or north-east). By examining the daily sequence of instantaneous difference fields (only day 2 shown here, see Fig. 21b), one can estimate the growth rate of this disturbance, which has a doubling time of about 15 hours in the first two days. A tendency of propagation downstream (towards the north-east) can also be observed, in accordance with the Rossby wave propagation in the lee of mountains as described in Grose and Hoskins (1979). The lee cyclogenesis phenomena is not, therefore, only a meso scale process confined to the

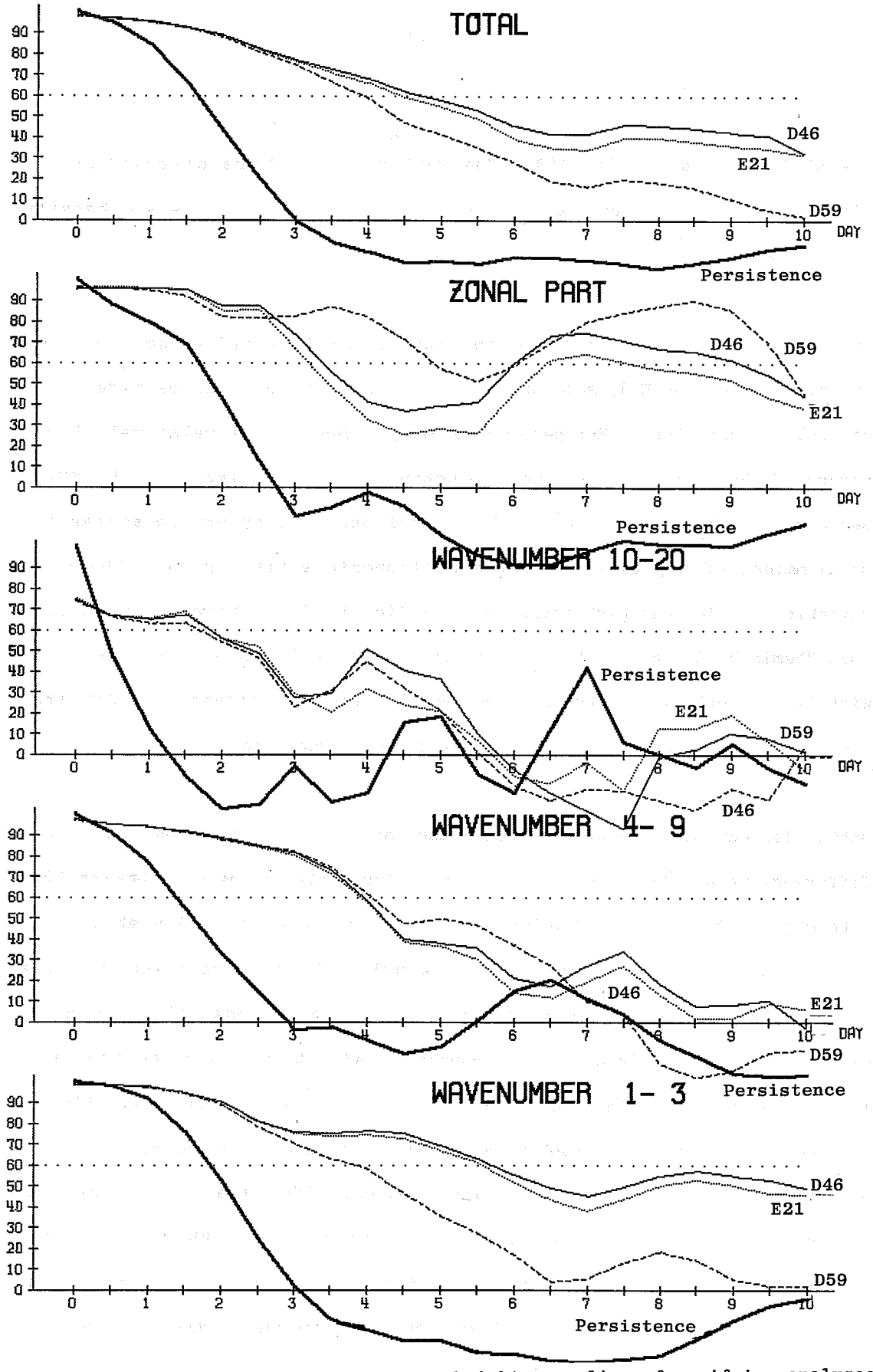

Fig. 20 Correlation coefficient between height anomalies of verifying analyses and various numerical experiments. Average between 20°N and 82.5°N and between 1000 and 200 mb. In addition to the total scores, a spectral breakdown is shown. Continuous thick lines: persistence forecast. Continuous thin line: D46, control experiment. Dotted lines: E21, enhanced Alps experiment. Dashed lines: D59, no mountains experiment.

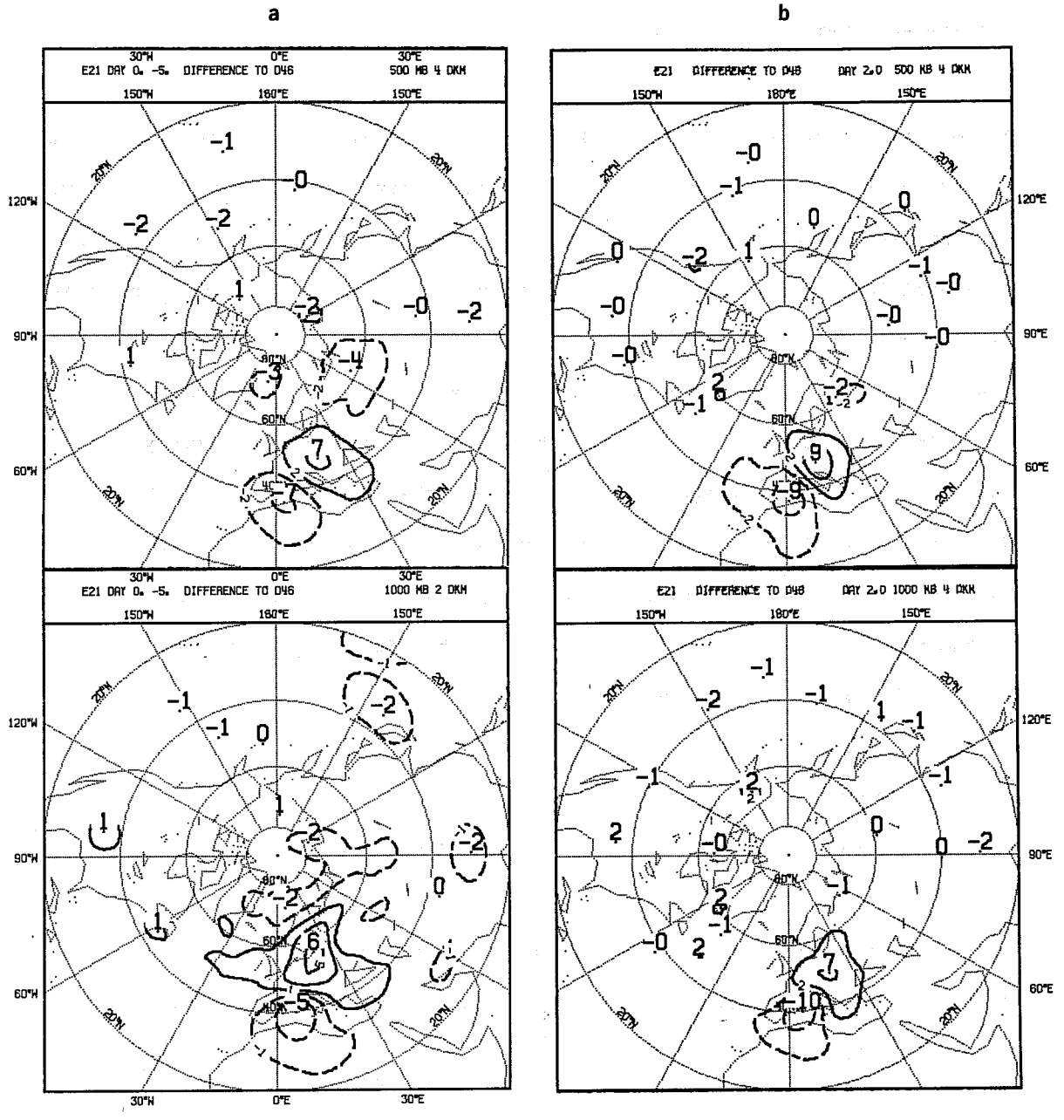

Fig. 21 (a) Day 0 to 5 mean difference map between experiment E21 (enhanced Alps) and experiment D46 (control).
Top: 500 mb geopotential height - lines every 4 dkm.
Bottom: 1000 mb geopotential height - lines every 2 dkm.

(b) As (a) but for day 2 only.

immediate lee of the Alps, but is part of a structured disturbance that affects the whole European region.

A comparison between Fig. 21a and Fig. 21b also highlights another important feature of the influence of the Alps. While at day 2 the disturbance shows no appreciable tilt with height (21b), the 5 day mean map (21a) shows a low-level doublet oriented NE-SW and an upper-level disturbance oriented almost N-S. This indicates that, while the linear orographic pertubation is essentially equivalent-barotropic, the interaction of such a forcing with a baroclinic "basic state" atmospheric flow develops structures (lee-cyclones) able to grow at the expense of the available potential energy of such a basic state and, therefore, baroclinic in nature. This supports the conclusions of Tibaldi, Buzzi and Malguzzi (1980) with results of a global model, not contaminated, therefore, by spurious lateral boundary conditions typical of limited area and channel models.

6. CONCLUSIONS

In summary, the following conclusions can be derived from the experiments:

1) It is confirmed that the Alps are responsible for the case of Mediterranean cyclogenesis under consideration, and participate to the control of its evolution in time.

2) This cyclogenetic effect is not simulated if the orography is "smoothed" in the model, as in the first version of the model used.

3) The same effect is, instead, obtained by simply increasing the height of the Alps to a realistic value that produces a blocking effect on the oncoming flow.

4) The difference fields between experiments with and without the Alps reveal

that the mountain induced perturbation, although initially barotropic, develops baroclinically in time. This perturbation is characterized not only by a depressionary field in the south-south-west of the barrier but also by a positive geopotential anomaly centre to the north-east of it. The horizontal extent of this induced perturbation is on the European scale and can, therefore, be reasonably considered as synoptically favourable to the onset of European blocking, which is often characterized by a positive geopotential anomaly over Northern Europe together with a negative anomaly over the Mediterranean.

5) Concerning the specific relationship between cyclogenesis in the lee of the Alps and blocking that originally prompted this investigation, these experiments are unfortunately not conclusive, chiefly for the reason that none of them predicts the onset of the blocking situation which follows the cyclogenesis with an accuracy sufficient to make them sensitive to the evolution of the previous synoptic development. More work is therefore needed to investigate this aspect.

6) The role of global orography in determining the onset of blocking and sustaining its maintenance is shown. The importance of orography as a principal source of quasi-stationary ultra-long waves is confirmed as well as the role of such waves in maintaining atmospheric blocking.

Acknowledgements

The authors are indebted to A. Speranza for numerous discussions that led to the formulation of this numerical experiment. The Italian Weather Service (Servizio Meteorologico dell'Aeronautica Militare) is gratefully acknowledged for partial support to this project under the form of computer time on the ECMWF computer system.

REFERENCES

Arakawa, A., 1966 Computational design for long-term numerical integration of the equations of fluid motion: two dimensional incompressible flow. Part 1. J. Comp. Phys., 1, 119-143.

Arakawa, A. and V.R. Lamb, 1977 Computational design of the basic dynamical processes of the UCLA general circulation model. Methods in Computational Physics, Vol. 17, J. Chang, Ed., Academic Press, 337 pp.

Arakawa, A. and W.H. Schubert, 1974 Interaction of a cumulus cloud ensemble with the large-scale environment. J. Atmos. Sci., 31, 674-701.

Austin, J.F. 1980 The blocking of mid-latitude westerly winds by planetary waves. Quart. J. Roy. Meteor. Soc., 106, 327-350.

Bengtsson, L. 1981 Numerical prediction of atmospheric blocking - A case study. Tellus, 33, 19-42.

Berggren, R., B. Bolin and C.G. Rossby, 1949 An aerological study of zonal motion, its perturbations and break-down. Tellus 1, 14-37 (1949).

Berkofsky, L. and Bertoni, E.A., 1955 Mean topographic charts for the entire earth. Bull. Amer. Meteor. Soc., 36, 350-354.

Bleck, R. 1977 Numerical simul8tion of lee cyclogenesis in the Gulf of Genoa. Mon. Wea. Rev., 105, 428-445.

Burridge, D.M. 1979 Some aspects of large scale numerical modelling of the atmosphere. Proceedings of ECMWF Seminar on Dynamical Meteorology and Numerical Weather Prediction, Vol. 2, 1-78.

Burridge, D.M. and J. Haseler 1977 A model for medium range weather forecasting - Adiabatic formulation. ECMWF Technical Report No. 4, 46pp.

Buzzi, A. and S. Tibaldi, 1978 Cyclogenesis in the lee of the Alps: A case study. Quart. J. Roy. Meteor. Soc., 104, 271-287.

Charney, J.G. and J.G. De Vore, 1979 Multiple flow dquilibria in the atmosphere and blocking. J. Atmos. Sci., 36, 1205-1216.

Charney, J.G. and D.M. Straus, 1980 Form-drag instability, multiple equilibria and propogating planetary waves in baroclinic, orographically forced, planetary wave systems. J. Atmos. Sci., 37, 1157-1176.

Egger, J., 1972 Numerical experiments on the cyclogenesis in the Gulf of Genoa. Beitr. Phys. Atmos., 45, 320-346.

Grose, W.L. and B.J. Hoskins, 1979 On the influence of orography on large-scale atmospheric flow. J. Atmos. Sci., 36, 223-234.

Hollingsworth, A., K. Arpe, M. Tiedtke, M. Capaldo and H. Savijärvi, 1980 The performance of a medium-range forecast model in winter - Impact of physical parameterizations. Mon. Weath. Rev., 108, 1736-1773.

Illari, L., P. Malguzzi and A. Speranza 1981 On breakdowns of the Westerlies. Geophys. Astrophys. Fluid Dyn., 17, 27-49.

Malguzzi, P. and A. Speranza 1981 Local multiple equilibria and regional atmospheric blocking. J.Atmos.Sci., 38, 1939-1948.

McWilliams, J.C. 1980 An application of equivalent modons to atmospheric blocking. Dyn. Atmos. Oceans, 5, 43-66.

Phillips, N.A. 1957 A coordinate system having some special advantages for numerical forecasting. J. Meteor., 14, 184-185.

Sadourny, R. 1975 The dynamics of finite difference models of the shallow-water equations. J. Atmos. Sci., 32, 680-689.

Temperton, C. and D.L. Williamson 1981 Normal mode initialization for a multi-level grid-point model. Part I: Linear aspects. Mon. Weath. Rev., 109, 729-743.

Tibaldi, S. 1980 Cyclogenesis in the lee of orography and its numerical modelling, with special reference to the Alps, in "Orographic effects in planetary flows", Editors, R. Hide and P. White, GARP Publ. Series No. 23, Chapter 7, pp. 207-232. WMO, Geneva.

Tibaldi, S., A. Buzzi and P. Malguzzi 1980 Orographically induced cyclogenesis: Analysis of numerical experiments. Mon. Wea. Rev., 108, 1302-1314.

Tiedtke, M., J-F. Geleyn, A. Hollingsworth and J-F. Louis 1979 ECMWF model-parameterization of sub-grid scale processes. ECMWF Technical Report No. 10, 46pp.

Trevisan, A. and A. Buzzi 1980 Stationary response of barotropic weakly nonlinear Rossby waves to quasi-resonant orographic forcing. J. Atmos. Sci., 37, 947-957.

Williamson, D.L. and C. Temperton 1981 Normal mode initialization for a multilevel grid-point model. Part II: Nonlinear aspects. Mon. Weath. Rev., 109, 744-751.

ECMWF PUBLISHED TECHNICAL REPORTS

No. 1 A Case Study of a Ten Day Prediction

No. 2 The Effect of Arithmetic Precisions on some Meteorological Integrations

No. 3 Mixed-Radix Fast Fourier Transforms without Reordering

No. 4 A Model for Medium-Range Weather Forecasting - Adiabatic Formulation

No. 5 A Study of some Parameterizations of Sub-Grid Processes in a Baroclinic Wave in a Two-Dimensional Model

No. 6 The ECMWF Analysis and Data Assimilation Scheme - Analysis of Mass and Wind Fields

No. 7 A Ten Day High Resolution Non-Adiabatic Spectral Integration: A Comparative Study

No. 8 On the Asymptotic Behaviour of Simple Stochastic-Dynamic Systems

No. 9 On Balance Requirements as Initial Conditions

No.10 ECMWF Model - Parameterization of Sub-Grid Processes

No.11 Normal Mode Initialization for a multi-level Gridpoint Model

No.12 Data Assimilation Experiments

No.13 Comparison of Medium Range Forecasts made with two Parameterization Schemes

No.14 On Initial Conditions for Non-Hydrostatic Models

No.15 Adiabatic Formulation and Organization of ECMWF's Spectral Model

No.16 Model Studies of a Developing Boundary Layer over the Ocean

No.17 The Response of a Global Barotropic Model to Forcing by Large-Scale Orography

No.18 Confidence Limits for Verification and Energetics Studies

No.19 A Low Order Barotropic Model on the Sphere with the Orographic and Newtonian Forcing

No.20 A Review of the Normal Mode Initialization Method

No.21 The Adjoint Equation Technique Applied to Meteorological Problems

No.22 The Use of Empirical Methods for Mesoscale Pressure Forecasts

No.23 Comparison of Medium Range Forecasts made with Models using Spectral or Finite Difference Techniques in the Horizontal

No.24 On the Average Errors of an Ensemble of Forecasts

No.25 On the Atmospheric Factors Affecting the Levantine Sea

No.26 Tropical Influences on Stationary Wave Motion in Middle and High Latitudes

ECMWF PUBLISHED TECHNICAL REPORTS

No.27 The Energy Budgets in North America, North Atlantic and Europe Based on ECMWF Analyses and Forecasts

No.28 An Energy and Angular-Momentum Conserving Vertical Finite-Difference Scheme, Hybrid Coordinates, and Medium-Range Weather Prediction

No.29 Orographic Influences on Mediterranean Lee Cyclogenesis and European Blocking in a Global Numerical Model